THESIS FOR THE DEGREE OF LICENTIATE OF ENGINEERING

Statistical Modelling of Lateral Vehicle Loads

MAGNUS KARLSSON

CHALMERS | GÖTEBORG UNIVERSITY

Department of Mathematical Statistics
Chalmers University of Technology and Göteborg University
SE-412 96 Göteborg, Sweden

Göteborg, November 2004

Statistical Modelling of Lateral Vehicle Loads
MAGNUS KARLSSON

© MAGNUS KARLSSON, 2004.

ISSN 0347-2809 / NO 2004:51
Department of Mathematical Statistics
Chalmers University of Technology and Göteborg University
SE-412 96 Göteborg
Sweden
Telephone + 46 (0)31-772 1000

Göteborg, Sweden 2004

Statistical Modelling of Lateral Vehicle Loads
MAGNUS KARLSSON
Department of Mathematical Statistics
Chalmers University of Technology and Göteborg University

Abstract

A way of describing lateral acceleration for fatigue assessments is discussed. The purpose of the model is to parameterise the different sources of the fatigue load, such as the operating environment and the influence of the driver. The measured lateral acceleration is modelled with an approximative curvature, and the average speed explaining centripetal acceleration in the curve. The difference between the model and the observed lateral acceleration (the residual) is further analysed. An algorithm for extracting the curvature is presented based on road construction requirements and suitable statistical distributions for different driving conditions are suggested. The algorithm is verified using proving ground measurements and video recordings in field. A regression model for the relation between the curvature and the chosen speed is investigated. The acceleration residual is modelled by a transformed normal process. For the model of the centripetal acceleration, explicit expressions for the expected cumulative fatigue damage and range spectrum using rainflow cycles are given. For the residual an upper bound for the expected damage is shown. Comparison between the modelled loads and observed loads are made in terms of cumulative fatigue damage and range spectra. The influence of different drivers and markets are discussed.

Keywords: Road curvature, driver influence, fatigue assessment, rainflow count

Acknowledgements

The research presented in this work has been financially supported by Volvo Truck Corporation and VINNOVA within its Swedish National Road Vehicle Program. This support is gratefully acknowledged.

My personal thanks goes to:

Thomas Svensson, my supervisor at FCC, for his great ability of bringing up new ideas, and all the interesting discussions about my research topic and many other topics.

Bengt Johannesson, my supervisor at Volvo Truck Corp., for his fantastic encouragement and support.

Jacques de Maré, my supervisor at the department of mathematical statistics, Chalmers University of technology, for his great efforts to create scientific environment to work in and helping me out with many scientific as well as practical details.

I would also like to thank, the other members of my supervising group, Pär Johannesson, FCC, Stefan Edlund and Inge Johansson, Volvo, for their many valuable comments.

Igor Rychlik also deserves special thanks for reading the manuscript of the second paper and supplying valuable comments, which greatly improved the paper. He also provided the ideas behind large parts of section 6 of the paper.

Thanks also to the people at the durability and reliability department at Volvo, the people at FCC, and the people at the department of mathematical statistics at Chalmers.

Finally, I would also like to thank my family and friends for their great support. And then, of course, Lisa, thanks for making my life so much better.

Göteborg, November 2004

Magnus Karlsson

Table of Contents

List of papers ..... **vi**

1. Background **1**

2. Sources for fatigue loads **2**

3. The lateral loads **4**
3.1 The curvature model 5
3.2 The speed model 6
3.3 The residual 6

4. The three objectives for lateral loads **7**
4.1 Classifying markets 7
4.2 Input signals for computer simulations 8
4.3 Test schemes 9

5. Conclusions **9**

6. Summary of appended papers **10**
6.1 Paper I: Driver Independent Road Curve Characterisation 10
6.2 Paper II: Parameterisation of Lateral Fatigue Loads on Vehicles 10

7. Future work **11**

References **11**

List of Papers

This thesis consists of the following papers:

Paper I: M. Karlsson, *Driver Independent Road Curve Characterisation*, presented at the IAVSD'03 conference, Aug 2003.

Paper II: M. Karlsson, *Parameterisation of Lateral Fatigue Loads on Vehicles*.

1. Background

The truck industry is increasingly characterised by specialisation and customerisation. This means that the vehicle's specification and equipment must be tailored to suit each particular transport mission. The main focus is to optimise the performance to give the customer optimal transport efficiency, that is to maximise productivity at the same time as the product cost is kept as low as possible.

The demands on transport efficiency, (loading capacity, fuel economy etc.) and environmental friendliness have thus created a trend in vehicle development towards lightweight constructions. However, when using lightweight constructions it is necessary to make sure that the demands on reliability and durability are maintained, especially since component failures may cause loss of performance. One of the major reasons for structural component failure is fatigue. Therefore it is of great importance to be able to predict what kind of loads (forces and moments) a particular truck will experience during its specified life, and to make sure that it does not break during this life. This task contains many difficulties. First of all the strength of the components varies due to variation in process and production, and secondly, and perhaps more importantly, there is a great variation of the loads depending on the application, the operating environment, the driver's behaviour and the vehicle's specification.

In order to relate the loads to the damage they cause the material, a cycle counting method can be used together with a damage accumulation model. This makes it possible to relate the loads to the fatigue life. The strength and the (accumulated) load can, from a probabilistic point of view, be considered two random variables, where failure of a component will occur if the load is greater than the strength (see Figure 1). This is a very simplified way of looking at the problem, but it has the great advantage of giving only one number explaining the damage situation, and it is thus useful for comparison. This is especially so here since one major interest is in comparing different markets with each other. However, to get to this one number, a model needs to be built up that gives a reasonable result and takes care of the built-in variations in the load. The task is naturally to design components that make the failure probability suitably small. In order to do this the designer needs knowledge about the strength and load variations.

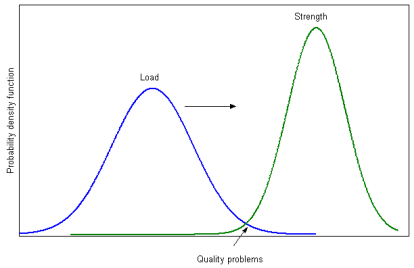

Figure 1. The accumulated load and the strength are seen as two random variables, where the accumulated load increases as time goes on. When the accumulated load is larger than the strength, failure will occur. It is necessary to keep the degree of failure at an acceptable level during the designed life.

The target of this project is to describe the loads. The traditional way of determining the loads has been to make field measurements of different applications. Since it is necessary to keep a very low failure rate, it is especially important to keep track of the vehicles that experience the most damage, or if seen in a more probabilistic sense, to understand the upper tail of the distribution. Therefore, with the intention of making the measurement damaging enough, many of the field measurements have been performed in such a way that the driver has been driving at a high speed over a bad stretch of roads. However, it is very unclear just how severe this driver and road are, and how this relates to the actual usage of a truck.

To guarantee that the truck will be strong enough, the systems and components are tested in rigs and full-scale tests are performed on proving grounds. However, the durability test tracks have often been constructed to replicate the worst-case loading conditions found during field measurements, and again it is therefore hard to relate this to actual customer usage. On the other hand, it is necessary to accelerate the proving ground tests, since the vehicle cannot be tested for as long a time as its life in field.

2. Sources for fatigue loads

To get a better understanding of the loads, measurements could be performed in such a way that the drivers and roads were picked randomly, but there are many markets and applications to cover and this would be a very time-consuming and expensive task. Furthermore, although past experience could be of great use, a new truck model with new features and components would naturally behave differently and therefore the loads would be different, and the process would have to be performed again for any new model. An alternative approach for how to get the fatigue load design specifications more related to the actual customer environment is to use questionnaire surveys, (see [1-3].), but these methods do not appear to be reliable enough, since they are based on a subjective judgement and the results are very sensitive to the type of questions asked.

A third alternative, the one that will be used here, can therefore be to start with the question: *What causes the loads?* As pointed out above there are several different factors that can be found:

1. *the operating environment*, that is the road condition that the truck will experience.
2. *the driver's behaviour*, such as speed changes and manoeuvring and yearly usage.
3. *the transport mission*, the particular usage of the truck.

Although in a sense a result of the three factors above, the actual *vehicle specification* will also affect the loads, for instance different sorts of suspension systems will give different kinds of loads.

If one could separate these different factors and describe them one by one, and understand the correlation between, for instance, the operating environment and the driver, much would be gained, since the description of the operating environment would hold for any truck. The same would probable be true to a great extent considering the driver's behaviour as well. It could therefore be of great interest to get a

parameterisation of the actual road conditions and then model how drivers behave on these roads. With such a description it would be possible to recreate the loads, and the increased understanding of the origins of the loads would lead to a better understanding of the markets and applications.

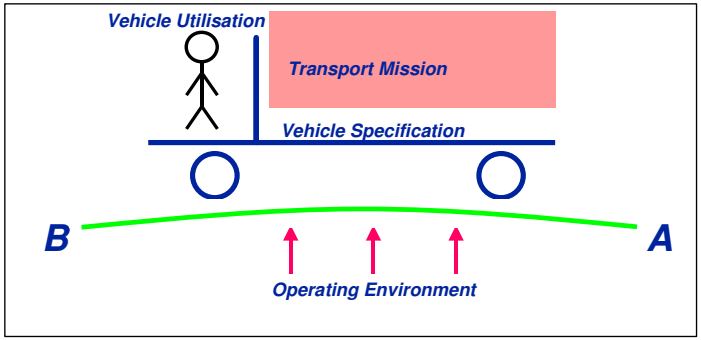

Figure 2. Different sources of fatigue load.

The purposes of this work is thus to create a model based on the principal of describing the different load origins one by one and then bring them together for a complete understanding of the loads.

In order to make such a description useful in practice some demands have to be fulfilled by the model. These demands can be summarised in the following way: It is necessary to be able to classify markets depending on the fatigue damage they cause. It must also be possible to use the model to generate input signals for computer models of a complete vehicle. Finally, there is a need to generate test schemes for test rigs.

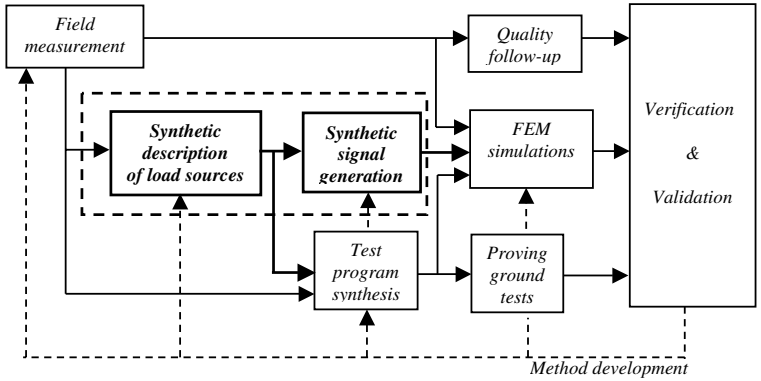

Figure 3. For a given market, the process of a balanced method development of synthetic descriptions of the load sources, the vehicle models for FEM simulations and the test programs. The parts where this project comes in are highlighted.

First, the model must be made in such a way that it is possible to compare different markets and applications to each other and to classify those markets and applications into different categories depending on how much fatigue damage they cause. The classification is necessary since it is becoming more and more important to tailor-make the trucks for their specific market and application. On the other hand, the developing cost increases with every new component, and therefore only a small number of classes can be considered.

Second, to be able to find such a classification computer simulations are indispensable tools. Finite element models can be used to simulate vehicle responses due to different excitations. To get a correct picture of the vehicle's performance it is necessary to have realistic input signals. A requirement for the model is therefore to provide realistic input signals for such complete vehicle models, which in their turn can be used to gather information about the classification. These input signals can, for instance, be in the form of a synthetic description of the road surface and the road curvature.

Third, it is necessary to be able to test whether a component is strong enough for the market and application it is going to be used. Tests are performed in different ways. The most common are rig tests and full-scale vehicle tests at proving grounds. The aim of these tests is to make sure that the great majority of the components, systems or vehicles will last their target life, which typically for a truck can be of the order 0.5-2 million kilometres.

The loads that the truck will experience on the road will have different origins; some will for instance be due to an uneven road surface while others depend on the curvature. It appears to be current practice to separate different kinds of load origins from each other, see [4,5]. Volvo's approach to the problem has been to describe different kinds of vehicle independent parameters called Global Truck Application (or simply GTA) parameters, see [6]. The aim of the GTA concept is to secure that the vehicles are specified, developed and sold with the same view of usage in mind.

The most important loads should be those coming from driving into potholes and bumps, road vibration, curvature, braking and accelerations. The potholes and bumps together with the road vibration is in GTA described as road condition and has been considered in a series of articles by Volvo, see [7-10].

3. The lateral loads

This work focuses on the lateral loads. In terms of durability arguably these loads, caused by curvature, are for most components not as damaging as those from the vertical loads [10], but will have a paramount influence on, for instance, steering components.

Ideally, the lateral acceleration (a_{lat}) can be calculated by using the centripetal acceleration, that is

$$a_{lat} = \frac{v^2}{r} \tag{1}$$

Knowing the radius (r) of the road and the speed (v) of the truck would then be enough to calculate the lateral acceleration, which in turn is proportional to the lateral force. However, the lateral acceleration will not only be affected by the actual curvature of the road, which the vehicle is driven on, but also the driver's way of taking the curve as well as his choice of speed will also be of great importance. Furthermore, the vehicle will affect the acceleration since the engine effect limits the top speed and the particular dampers used affect to what degree potholes and bumps will cause lateral loads. To understand the lateral acceleration it is therefore necessary to describe these different effects. Thus a parameterisation of the radius, the speed, and the driver's behaviour as well as the behaviour of the vehicle when driving on the road is desirable.

3.1 The curvature model

When constructing a road curve a crucial part is to make sure that vehicles driving through the curve will not experience too high lateral acceleration. In order to avoid this and to get a smooth ride through the curve it is therefore common to construct a constant curve radius over a longer time, say a couple of seconds. Thus if the driver uses the same speed through the curve the acceleration will be constant. (See eq. 1.) One way of modelling a curve would therefore be to think of it as having a constant radius over the entire curve. However, if the curve is narrow, i.e. has a small radius, it is probably better to have an area at the beginning (and the end) of the curve where the radius is adapted to the part with a small constant radius. Thus it would be easier for a driver to adjust to the smaller radius.

The Swedish National Road Administration [10] constructs curves according to the following concepts: If the radius is big (at least 900 m on a major road), the curve should follow the arc of a circle, i.e. has a constant radius. If the curve is narrow it should first have a linear change of the curvature, then the radius stays constant for a certain time and finally increases again until the road is straight.

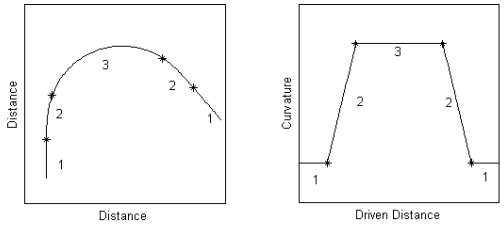

Figure 4. To the left: A straight part before entering the curve (1), an adaptation area where the radius decreases (2), and an area of constant radius (3). To the right: The curvature for the same curve.

According to these ideas it is therefore reasonable to see the curvature, here defined as the inverse of the radius at any point of the road, as following a trapezoid. See Figure 4 above. Since the actual radius of the road cannot be directly measured in field measurements, it is necessary to make an estimate of this entity. This can be done using the trapezoid model. With a suitable way of estimating the curvature from the measurements it is possible to describe a road curvature as a distribution of trapezoids. The parameters of the trapezoid can be described through a statistical distribution. This then provides the description of the operating environment.

3.2 The speed model

To get a complete understanding of the loads it is, as pointed out above, also necessary to model the driver's behaviour. In terms of curves, this means the speed at which he drives through the curve, and his ability to follow the exact curve. Since the lateral acceleration depends on the radius and the speed, it seems reasonable that there is a relation between the radius and the choice of speed in the curve. It is most likely a good idea to choose a lower speed when driving in a narrower curve. The proposition in this work of how to model this relation is to use a regression model to describe, for instance, the mean speed of the truck in the curve.

3.3 The residual

However, even with a description of the relationship between the driver's choice of speed and the radius of the curve, we cannot fully describe the measured lateral acceleration. As pointed out above the lateral acceleration that the truck will experience will also be affected by the driver's ability to follow the real curve, the unevenness of the road, and the effects of the vehicle, etc. These different effects can be seen as a residual. One part of this can be explained by a simple measurement error, which can be seen as a high-frequency component. The driver's influence, such as over-compensating when taking the curve, can be regarded as a low-frequency component. Other possible factors causing errors are disturbances from potholes and road roughness, the dynamics of the vehicle, the effects of the velocity, and the surrounding traffic. Thus, it should be possible to model the measured lateral acceleration (a_{meas}) as coming from two random processes, one corresponding to the trapezoids (a_{trap}) from the curvature model (C_{trap}) together with the speed model (v), which is zero during the straights and one corresponding to the residual (a_{res}), where the residual is a combination of the factors mentioned above:

$$a_{meas}(t) = a_{trap}(t) + a_{res}(t) = v^2(t) C_{trap}(t) + a_{res}(t) \tag{2}$$

$$a_{res}(t) = \delta_{driver}(t) + \delta_{measure}(t) + \delta_{road}(t) + \delta_{vehicle}(t) + \delta_{velocity}(t) + \delta_{surround}(t) \tag{3}$$

The first part (a_{trap}) could then be seen as the acceleration that the vehicle would have experienced if the driver had followed the road exactly.

The residual (a_{res}) could possibly be divided into one part corresponding mainly to the driver's behaviour and one part mainly corresponding to the vehicle. This can be done

by running the trapezoid signal (a_{trap}) through a simple vehicle model and study the effects of the model to see what part of the residual that the vehicle is responsible for. Naturally the driver takes into consideration the vehicle responses, but studying the problem as an open loop problem will still lead to some understanding of the loads, not least when it comes to understanding the frequency content.

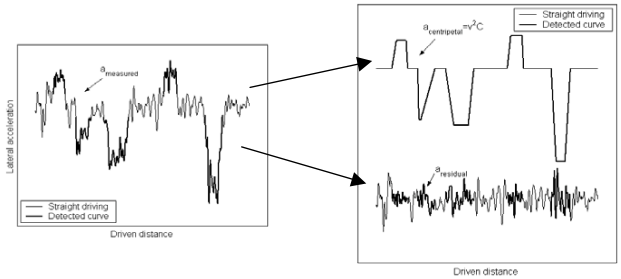

Figure 5. The separation of the measured lateral acceleration into two different parts, one corresponding to the fitted trapezoids and one corresponding to the residual.

4. The three objectives for lateral loads

The three objectives that we need to fulfil in order to have a useful model is as pointed out above, (1) to be able to classify markets depending on the fatigue damage they cause, (2) to generate input signals for computer models of a complete vehicle and (3) to generate test schemes.

4.1 Classifying markets

To fulfil the first of the three demands above, it is necessary to find a suitable way of differentiating between the classes. The factor that is most often used to measure the fatigue wear is the accumulated fatigue damage. Thus, threshold values for the accumulated fatigue damage are necessary to make a distinction between the different classes. The model for the acceleration must therefore be converted to accumulated fatigue damage. In this conversion it is still of interest to keep the separation between the effect of the driver and the effect of the road, this is since it brings the possibility of comparing the effects of the drivers in different regions. In this work the following approximation for the measured damage will therefore be used:

$$D_{meas} \approx D_{trap} + D_{res} \tag{4}$$

where

$$D_{meas} = D\left(a_{meas}(\cdot)\right) \tag{5}$$

$$D_{trap} = D\left(a_{trap}(\cdot)\right) \tag{6}$$

and

$$D_{res} = D\left(a_{res}(\cdot)\right) + D\left(\hat{a}_{trap}(\cdot)\right) - D\left(a_{trap}(\cdot)\right) \tag{7}$$

where $D\left(x(\cdot)\right)$ is the damage caused by the process $\{x(t)\}$, $\hat{a}_{trap}$ is the maximum acceleration over each curve, i.e. the acceleration coming from the trapezoid model of the curvature plus the maxima of the residual over that curve. The "trapezoid damage" is the damage caused by the trapezoid process, and the "residual damage" is the damage caused by the residual process together with a correction term which takes into consideration the fact that the highest peaks will be caused by both the trapezoids and the residual. The maximum value of the residual over each curve is modelled as an exponentially distributed variable.

To compare two different applications that are affected by randomness with each other, a natural measure is the expected damage, that is by knowing the distribution of the damage one can calculate the expected value:

$$\mathbf{E}[D_{meas}] \approx \mathbf{E}[D_{trap}] + \mathbf{E}[D_{res}] \tag{8}$$

Since the distributions available in the model focus on the accelerations rather than the damage, an approximation has to be made in a suitable way. For $\mathbf{E}[D_{trap}]$ and $\mathbf{E}[D(\hat{a}_{trap}(\cdot))]$ it is possible, using the parameterisation of the curvature trapezoids, the speed model and the model for the maximum value of the residual, to calculate the expected damage. The model for approximating the expected value of the damage for the residual process, i.e. $\mathbf{E}[D(a_{res}(\cdot))]$, is due to Rychlik [12].

4.2 Input signals for computer simulations

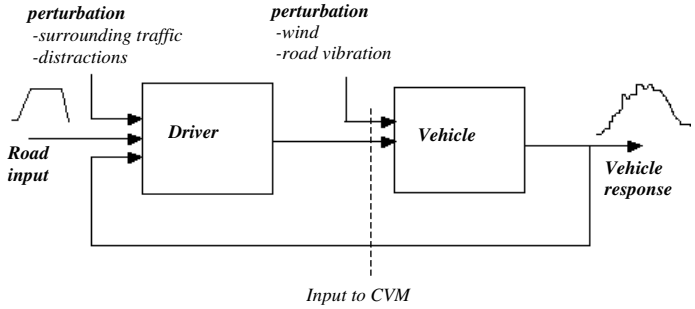

Figure 6. Control loop for the driver vehicle relation. The dotted line is where the input to the complete vehicle model is performed.

The second objective is to be able to generate reasonable input signals for finite element models (FEM) of complete vehicles. A necessary input parameter for the FEM is the wheel angle. The driver-vehicle relation is seen as a control loop, where the actual road the driver should follow (here represented as a trapezoid) is perturbed by the vehicle, the surrounding traffic and other sources of distraction. Then the driver's way of turning the wheel is also distorted due to such factors as wind and road vibration. (See Figure 6 above.)

The wheel angle can be calculated when knowing the curvature of the path that the truck is driven on through the following equation:

$$\theta(t) = \arcsin\left(\frac{L}{R(t)}\right) \tag{9}$$

where (L) is the length between the front axle and the middle of the rear axles. The radius (R) in the equation can be found using eq. (10).

$$R(t) = \frac{1}{C(t)} = \frac{1}{C_{trap}(t) + \frac{a_{res}(t)}{v^2(t)}} \tag{10}$$

If the truck has a boogie, eq. (9) and (10) are somewhat shifted: in this case L denotes the distance from the front axle to the boogie. A good input signal for the CVM can therefore be created using the distributions of the curvature and a model for $a_{res}(t)$.

4.3 Test schemes

The third objective of the model is to create test schemes for components sensitive to the lateral loads. The two main sources of variation in the loads are firstly the markets and the applications in which the vehicle is going to be used and secondly the drivers who drive the vehicle. Thus knowing the joint distributions of these two features it would be possible in theory to find an exact test spectrum for a certain customer, for instance the 99%-customer. However, in the model above the joint distribution is not available, but rather the marginal distributions for the curvature, a model for the relation between the speed chosen and the curvature and a description of the residual. (See Figure 7 below.) Thus it is possible to find a certain customer when only considering, for instance, the curvature variation or only the driver variation, but not for the combined effects. However, a damaging enough customer will be found when combining the 99%-effect of the curvature as well as the driver.

5. Conclusions

The model for the lateral accelerations is built up by three elements: the curvature distributions, which describe road conditions, the speed model, which describes how the driver chooses the speed, and finally the residual, which has several different sources, but whose major influences should be the driver's response to other factors than the road as well as vehicle dynamics.

The model is worked out so that it makes it possible to calculate the fatigue damage from the parameters and to separate the damage effect of the road and speed from the effect of the residual. As discussed above it is also possible to use the model as input data for a complete vehicle simulation.

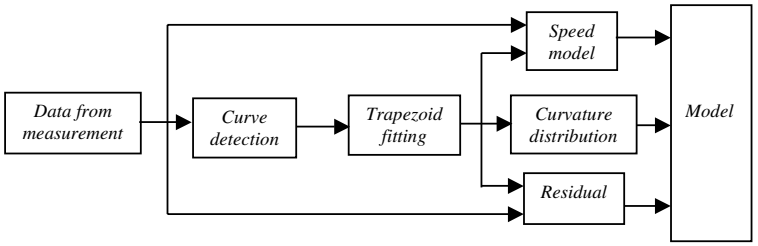

Figure 7. The model for the synthetic description of the measurement is built up from a description of the curvature, a model for the speed chosen while driving in curves and a model for the acceleration residual.

6. Summary of appended papers

6.1 Paper I: Driver Independent Road Curve Characterisation

The method of determining the statistical distribution of curvature of road curves is presented. An algorithm for detecting curves from measurements is explained and verified through proving ground measurements and video recordings from field measurements. It is explained how the trapezoids can be fitted to the curvature signal, and why a trapezoid is a reasonable model. The method is verified against proving ground measurements and applied to a series of measurements in Brazil with different drivers on the same road. The distributions of the curvature for the different drivers are presented.

The residual discussed here is the curvature residual, i.e. the difference between the measured curvature and the fitted trapezoids. The variance of the residuals in the curves is used to compare the effects of different driving styles. The measurements are the same as above with different drivers on the same road.

6.2 Paper II: Parameterisation of Lateral Fatigue Loads on Vehicles

In this paper the curvature model is discussed again and suitable distributions for city driving as well as highway and secondary roads are suggested. A model for the relation between the curvature and the speed chosen is investigated. A model for the acceleration residual, which assumes that the residual is a transformed normal process, is also given. The residual is independent of the other parameters.

With these models it is possible to make an approximate calculation of the expected accumulated fatigue damage for the different parts of the measured lateral acceleration.

The curvature model and the model for the speed provide a distribution for the lateral accelerations created when driving in curves. For the model of the centripetal acceleration an explicit expression for the expected cumulative fatigue damage using rainflow cycles is given, and expressions for the range spectrum is shown. For the residual an upper bound for the expected damage is shown. Comparison between the modelled loads and observed loads are made in terms of cumulative fatigue damage and range spectra. Finally, the influence of different drivers and markets are discussed. Most of the proofs of the theoretical results are found in the appendix

7. Future work

The above model gives little insight into the residual. It is of great interest to understand what part of the residual comes from the effects of the vehicle, and what part is due to other effects such as the driver. One way of studying this is to use simple computer models of vehicles with trapezoid signals as input. This would give reasonable responses in terms of power spectral densities.

Another interesting aspect is to include the proportion of two curves in the same direction in the model for the trapezoid acceleration. There might also be a possibility to find at least an asymptotic variance for the damage, and model the amount of curves as a Poisson process, which would give an increased understanding for the variability.

An important step is also to adapt the model to on-board logging, which makes it possible to log much larger amounts of data than what is currently possible.

A fourth interesting aspect would be to study the effects of different drivers more closely in order to see to if it is possible to find a statistically significant difference between the drivers. In the same way it would be of great interest to study different markets. Another interesting part to be investigated is the robustness of the model. Finally it would of course be of great interest to extend the concept to other loads such as those coming from the topography of the road, and naturally also to continue the work with vertical excitations such as potholes and road vibration.

References

1. Olofsson, M.: *Evaluation of Estimates of Extreme Fatigue Load – Enhanced by Data from Questionnaires*. Licentiate of Engineering Thesis, Chalmers University of Technology, Göteborg, Sweden, 2000.
2. Niemand, L.: *Probabilistic Establishment of Vehicle Fatigue Test Requirements*. Master of Engineering Thesis, University of Pretoria, Pretoria, 1996.
3. Thomas, J.J., Perroud, G., Bignonnet, A., Monnet, D.: Fatigue Design and Reliability in the Automotive Industry. In Marquis, G. Solin, J. (editors), *Fatigue Design and Reliability, ESIS Publication 23*. Oxford, UK: Elsevier Science, pp.1-12, 1999.
4. Grubisic, V., Fischer, G.: Methodology for Effective Design Evaluation and Durability Approval of Car Suspension Components. *SAE Technical Paper 970094*, 1997.
5. Fischer, G.: Design and Quality Assurance of Vehicle Components based on the Usage Related Stress Analysis. *XXIX Convegno Nazionale dell´Associazione Italiana per l'Analisi delle Solleciatazioni*, Lucca, 6-9 Sept. 2000.
6. Edlund S., Fryk P.O.: The Right Truck for the Job with Global Truck Application Descriptions, *SAE Technical Paper 2004-01-2645*, 2004.

7. Aurell J., Edlund S.: Operating Severity Distribution a Base for Vehicle Optimization, *11th IAVSD-Symposium on the Dynamics of Vehicles on Roads and Tracks*, Kingston, Canada, 1989.
8. Aurell J., Edlund S.: Prediction of Vibration Environment in Real Operations Described by Q-distributions, *14th IAVSD - Symposium on the Dynamics of Vehicles on Roads and Tracks*, Ann Arbor, USA, 1995.
9. Öijer, F., Edlund S.: Complete Vehicle Durability Assessments Using Discrete Sets of Random Roads and Transient Obstacles Based on Q-distributions, *17th IAVSD - Symposium on the Dynamics of Vehicles on Roads and Tracks*, Lyngby, Denmark, 2001.
10. Öijer, F., Edlund S.: Identification of Transient Road Obstacle Distributions and Their Impact on Vehicle Durability and Driver Comfort, *18th IAVSD - Symposium on the Dynamics of Vehicles on Roads and Tracks*, Atsugi, Japan, 2003.
11. Vägverket: Vägutformning-94 version S-1, del 6 Linjeföring. *Vägverket Publikation 1994-52*, Borlänge, 1994. (In Swedish).
12. Rychlik, I. Rainflow Cycles, Markov Chains and Electrical Circuits, In Spencer, B.F., Johnson, E.A., Balkema, A.A. (editors), *Stochastic Structural Dynamics*, ISBN 90 5809 0248, pp. 229-234, 1999.

Driver Independent Road Curve Characterisation

MAGNUS KARLSSON[1]

SUMMARY

A method to determine the statistical distribution of curvature of road curves is presented. The curvature is the inverse of the radius at any point. From road construction requirements it is reasonable to model the curvature of a road curve with a trapezoid. The algorithm presented detects curves from measurements and fits a trapezoid to each curve. The residual between the fitted trapezoid and the measured curvature can be seen as the driver influence. The method is verified against proving ground measurements and applied to a series of measurements in Brazil with different drivers on the same road. The distributions of the curvature for the different drivers are presented and the variance of the residuals in the curves is used to compare the effects of the different driving styles.

1 INTRODUCTION

A major problem when predicting fatigue life for vehicle components is to determine the service loading conditions that the vehicle will experience during its life. Due to insufficient knowledge about the loading conditions the strength of components are often exaggerated through high safety factors. Many of these unnecessarily strong constructions can be avoided with a better understanding of the fatigue load in the real operating environment. The natural way to acquire information about the service loading is to make field measurements of forces, strains etc. However, it is a troublesome and expensive task, especially since there exists a great variation between different customers' way of using their vehicles.

Since the field measurements have seldom been considered long enough they have often been performed in such a way that the driver has been driving at high speed over a bad road stretch, thus guaranteeing that the measurement is severe enough. In the same way the durability test tracks have been constructed to replicate the worst-case loading conditions found during field measurements. [1]

There are other suggestions for how to get the fatigue load design specifications more related to the actual customer environment, by using for instance questionnaire surveys, (see [1-3].), but these methods do not appear to be reliable enough.

[1] *Address correspondence to:* Volvo Truck Corporation, Department 26780 A2, SE-40508 Göteborg, Sweden. Tel.: +46 31 668 286; Fax: +46 31 508 764; E-mail: magnus.k.karlsson@volvo.com

In recent years, the ambition in the automotive industry has been to design and optimise components towards a finite fatigue life. This optimisation has been based on the almost opposing requirements of lightweight design on one hand and safety and durability requirements on the other hand. It has become obvious that a more thorough understanding of the complex fatigue loading conditions is necessary.

Most techniques today directly try to describe the loading conditions in terms of forces and moments. It appears to be practice of the date to separate different kind of load origins from each other, see [4,5]. The most important loads should be those coming from driving into potholes and bumps, road vibration, curvature, braking and accelerations. These can be seen as vertical, lateral and longitudinal load origins. The vertical loads have been considered in a series of articles by Volvo, see [6-8]. This particular work focuses on the lateral loads. These loads, caused by curvature, are arguably not as great as those from the vertical loads, but will have a huge influence on, for instance, steering components.

This article will in section 2 describe a new concept for describing loads based on separation of the effects of the operating environment, driver's influence, transport mission and the vehicle design. These ideas will then be applied to lateral loads. In section 3 a mathematical description of a curve is suggested, based on road construction requirements. In section 4 an algorithm for detecting curves from measurement is described and the mathematical description of a curve is used to find the curvature for each detected curve. These methods are verified against proving ground measurement. In section 5 the ideas are applied to measurements in Brazil. The distribution of curvature is found. In section 6 some conclusions about the method are drawn.

2 A CONCEPT FOR DESCRIBING LOADS

An alternative to the idea of trying to describe the loads directly, is to ask the interesting question: "What causes the loadings?" Naturally there are several factors, but the most important should be the following:

- The operating environment: What kind of roads is the vehicle driven on?
- The vehicle utilisation: How is the driver driving the vehicle?
- The transport mission: What is the vehicle used for?
- The vehicle design: What kind of vehicle do we have?

An idea could therefore be to describe these factors separately, in order to actually understand from where the loads come, and how important the above listed sources are. The main purpose of this idea is to separate the description of the road from the influence of the driving style, the vehicle design and the effects of surrounding traffic. This means that the road description will be approximately the same irrespective of the driver and at what time the measurement is performed. The

description of today will therefore hold in the future as well. The influence of driving style can then be described separately. The method therefore gives an opportunity to study to what extent the driver influence affects the fatigue life. This can then be compared to the influence of the market where the truck is used as well as the mission of the truck. The description of the operating environment can also be of great use when performing handling and comfort analyses.

3 A SIMPLE MATHEMATICAL MODEL OF A CURVE

When constructing a curve a crucial part is to make sure that vehicles driving through the curve will not experience too high lateral accelerations. In order to avoid this and to get a smooth ride through the curve it is therefore useful to have a constant curve radius over a longer time, say a couple of seconds. One way of modelling a curve would therefore be to think of it as having a constant radius over the entire curve. However if the curve is narrow, i.e. has a small radius, it is probably better to have an area at the beginning (and the end) of the curve where the radius is adapted to the part with a small constant radius. Thus it would be easier for a driver to adjust to the smaller radius.

The Swedish National Road Administration [6] constructs curves according to the following concepts: If the radius is big (at least 900 m on a major road), the curve should follow the arc of a circle, i.e. has a constant radius. If the curve is narrow it should first have a linear change of the curvature, then the radius stays constant for a certain time and finally increases again until the road is straight.

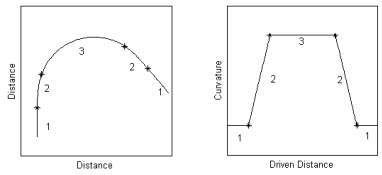

Fig. 1. To the right: A straight part before entering the curve (1), an adaptation area where the radius decreases (2), and an area of constant radius (3). To the left: The curvature for the same curve

According to these ideas it is therefore reasonable to see the curvature, here defined as the inverse of the radius at any point of the road, as following a trapezoid. See Fig. 1 above.

An equation for the trapezoid model used in this paper is as follows:

$$C(x) = \begin{cases} k \cdot (x - (x_0 - l)), & x_0 - l \le x < x_0 - l + h/k \\ h, & x_0 - l + h/k \le x < x_0 + l - h/k \\ k \cdot (x_0 + l - x), & x_0 + l - h/k \le x \le x_0 + l \end{cases} \quad (1)$$

where k is the slope of the side of the trapezoid, x_0 is the distance from the starting point of the road, l is the distance from the middle of the curve to the endpoints, and h is the height of the trapezoid. (See Fig. 2.) The trapezoid is assumed to have the same slope on both sides.

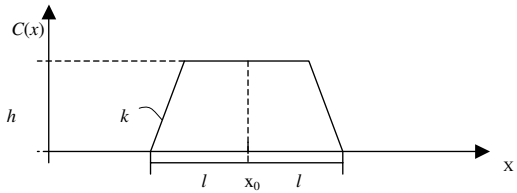

Fig. 2 A trapezoid with the parameters in the model.

4 DETECTING AND MEASURING CURVES

4.1 Different Driving Modes

Before it is possible to use real measurements to analyse the curvature of a road with the above-mentioned trapezoid method, two problems have to be solved. First we have to know where there is a curve. That is, we have to be able to automatically detect a curve simply by running the measurements through a programme. Second, we have to use the measurements to somehow estimate the curvature, where we have detected a curve.

The problem of detecting the curves can be solved in the following way. Each point of the measurements is sorted into any of the following three categories: *manoeuvres*, *curves* and *straights*. The term manoeuvres is in this case for instance parking manoeuvres or reversing for loading or unloading. The differentiation can

be made in the following way. Manoeuvres are characterised by high wheel angle and low speed. Thus the measurement is searched for points fulfilling these demands. Secondly the measurement is searched for characteristics for curves such as high lateral acceleration under a certain time, and high speed relative to the manoeuvres. What remains after these two searches is considered to be straight parts.

4.2 An Estimate of the Curvature

The curvature of the road can be found using measurements in which the yaw rate and the velocity have been recorded. The curvature can be estimated by the ratio of the yaw rate and the velocity at any point. Naturally these measurements will not exactly follow a trapezoid for each curve and then stay zero for the straights. The idea is instead that the curvature can be described as a sum of a deterministic function and a zero mean random process. The deterministic function corresponds to the trapezoid and the random process to the residual between the actual measurement and the trapezoid fit.

In practise, the trapezoid fit is made in the following way. For every curve detected, the signal corresponding to the curvature is picked out, and the distance driven is found by integrating the velocity for this particular part of the road. A trapezoid as a function of the driven distance is fitted to the measured curvature.

Under the assumption that we get the true curvature from the measurement above, how do we then explain the residual? One part can be explained by a simple measurement error. This can be seen as the high-frequency component. The low-frequency component on the other hand can be regarded as the driver's influence, such as over-compensating when taking the curve. Other possible factors causing errors are disturbances from potholes and road roughness, the dynamics of the vehicle, and the velocity. It should be possible to model the curvature (C) as a deterministic function corresponding to the trapezoids ($C_{trapezoid}$) and a stochastic process corresponding to the residual (δ), where the residual is a combination of the factors mentioned above:

$$C = C_{trapezoid} + \delta = C_{trapezoid} + \delta_{driver} + \delta_{measure} + \delta_{road} + \delta_{vehicle} + \delta_{velocity} \qquad (2)$$

4.3 Reference Measurements and Verification of the Algorithm

The way of detecting curves from the measurement is naturally based on a great deal of subjective judgement. Questions like: "What is low speed?" can of course be raised. In order to verify that the method actually works, the separation of the measurement was compared to the actual situation on the road by studying video

films, which were recorded simultaneously with the measurements, as well as comparing the result with known curves at a proving ground.

The result was that it is possible to use this sort of decomposition. On the proving ground measurements, two very small curves that did not exist according to the map were detected out of a total amount of thirty-five curves. On the other hand all existing curves were detected. Since the decomposition is based on threshold values there is of course a small number of questionable cases. The most sensitive part is whether or not over-turns and such things as turning in order to avoid potholes should be considered as curves or not. In this study most of them are not. The key is how long time it should take to drive through a curve. Making this parameter smaller places the above two examples in the class of curves.

In order to verify that the method of fitting a trapezoid to each detected curve works, measurements from a proving ground with known curvature were used. The error from the measurements were found in the following way:

$$\varepsilon = \frac{r_{fitted} - r_{true}}{r_{true}} \qquad (3)$$

where r_{fitted} is the smallest radius found in each curve, and r_{true} is the radius according to a map of the proving ground. The program was run over a series of such measurements, containing altogether thirty-five curves. The mean error was very close to zero (-0.0033) and thus it seems like r_{fitted} is an unbiased estimate of r_{true}. The standard deviation of ε was found to be 0.054. To better understand these figures estimating a $r_{fitted} = 90m$ when $r_{true} = 100m$ gives an error $\varepsilon = 0.10$. Thus it seems like the estimate is good, especially if we consider the fact that the drivers do not necessarily follow the track of the road exactly, but may very well try to take a somewhat shorter way through a curve, or may have to take a longer way due to the surrounding traffic.

Another way of verifying the algorithm is to use the measurement of the curvature to find the road driven and compare that to the road that is found by using the fitted trapezoids. Although this is not the purpose of this model it should give a good hint about the quality of the model. The results come from a measurement in Brazil. As can be seen in Fig. 3, there is a rather small difference between the two estimated roads. The difference appears about halfway through the road, where the trapezoid method gives a less emphasised curve to the left than the original measurement, which is then propagated through the rest of the measurement. At the very end of the road there is also a clear mistake. Nevertheless the results seem to verify the quality of the trapezoid model. It would be of interest to compare the resulting roads curve by curve, but since the original measurement contains no information on exactly where the curves are located such a direct comparison is not

possible. It is therefore difficult to draw any further conclusions more than that it looks as if the maps are very similar.

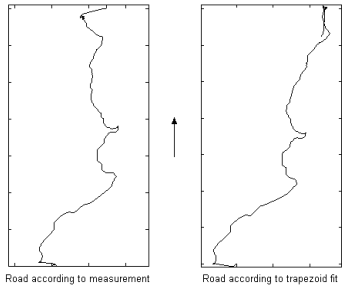

Fig. 3. The road according to the measurement and according to the fitted trapezoids. The arrow indicates the direction in which the truck was driven.

4.4 The Residual

As a first idea for a measure of the drivers' unsteadiness, the variance of the residuals in the curves can be used, thus giving us a possibility to compare the different drivers to each other. An unsteady driver gives a high variance, which will cause more damage.

5 METHOD APPLIED TO MEASUREMENTS IN BRAZIL

5.1 Description of Measurements

A series of measurements performed in Brazil was used to try out the suggested method. During these measurements five different drivers were driving the same route consisting of approximately 25 km highway, 25 km secondary road, 7 km unpaved road and 2.5 km city driving. One of the drivers was driving the stretch of roads four times, in order to see how great the variation for a single driver is.

According to the trapezoid model it should be possible to estimate the curvature of the road at every point by fitting a trapezoid to the measured curvature where a

curve has been detected. Thus when letting different drivers driving over the same route the results of the estimated curvature should, at least approximately, be the same.

The algorithm described above was used to detect curves and estimate the curvature of each detected curve for all eight measurements. Since the route was not exactly the same (some drivers skipped the city driving or parts of it), some of the most obvious curves were not included for all measurements. Nevertheless, it is still possible to study the empirical distribution of, for instance, the curvature or the curve length, which should be the same for all drivers.

5.2 Results from Measurements

In Fig. 4 the empirical distributions for the curvature for the five different drivers are plotted. As a reference the empirical distribution from another measurement performed in Brazil is also plotted. This measurement was 57 km long and consisted mainly of secondary and unpaved road. In Fig. 4 it is referred to as "reference road".

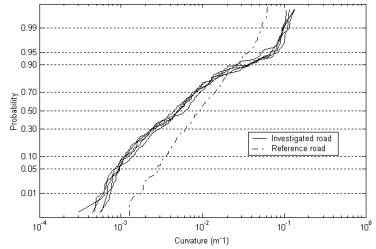

Fig. 4. Empirical distribution for the curvature for different measurements on the same road as well as a reference measurement on another road. (Plotted on lognormal paper.)

In the upper right corner of the figure an area can be seen where the distribution for the investigated road makes a bend. This part corresponds to the city driving part where the curves are narrow and similar in terms of curvature. On the other hand, in the left part of the figure the investigated road gets lower values on the curvature, than the reference road. This part comes from the highway section where the curves are designed to make it possible to drive fast. The reference road has a more homogeneous distribution of curves.

Since not all drivers took the same route the city driving part was excluded when comparing the residuals. The variance of the residuals in the remaining curves was

recorded. In Fig. 5 the variance of the residuals for the different drivers are shown normalized by the highest value. Driver No. 5 drove the route four times.

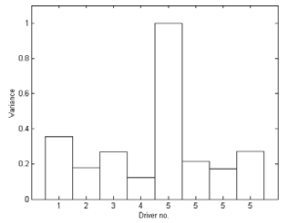

Fig. 5. The variance of the residuals for the different drivers normalized by the highest variance.

5.3 Discussion on the Results

The results from the Brazilian measurements indicate that it is possible to use the detection algorithm and the trapezoid method to measure the curvature on the roads with a fairly high precision. The empirical distributions for different drivers appear to be very similar from one driver to another, and can thus be seen as driver independent.

A co-driver from Volvo made a subjective judgement on the different drivers, which makes it possible to check the result from the variance of the residuals.

Table 1. The subjective judgement of a co-driver (a Volvo employee).

Driver no:	1	2	3	4	5
Judged as:	Fast and somewhat reckless	Fast and experienced	Careful	Careful	Fast
Nationality:	Brazilian	Brazilian	Brazilian	Brazilian	Swedish

A comparison shows that the reckless driver has the second highest variance, although he was acquainted with the course. The Swedish driver was not familiar with the Brazilian conditions during his first measurement, which is shown clearly. In the following measurements he is on the same levels as the Brazilian drivers. Notable is that one of the “careful” drivers (No. 3) did not get a very low value.

6 CONCLUSION

The results indicate that it is possible to use the above-suggested ideas to detect the curves and measure the curvature on the roads with a fairly high precision. This gives us a useful tool to detect the road conditions which is easy to use in, for instance, complete vehicle models.

The residual gives us information about to what extent a driver is driving unsteady. Thus we can find a bad driver by looking at the residual. However it should be pointed out that the most severe effect on fatigue life is the vehicle speed.

7 ACKNOWLEDGEMENTS

This work has been a joint work between Volvo Truck Corporation, Fraunhofer-Chalmers Research Centre for Industrial Mathematics (FCC), and the Department of Mathematical Statistics at Chalmers University of Technology, where the author is a graduate student. The author wishes to express his gratitude towards his supervisors Dr. Thomas Svensson, FCC, Prof. Jacques de Maré, Chalmers and Dr. Bengt Johannesson, Volvo. The project is funded by the Swedish Agency for Innovation Systems.

REFERENCES

1. Olofsson, M.: *Evaluation of Estimates of Extreme Fatigue Load – Enhanced by Data from Questionnaires*. Licentiate of Engineering Thesis, Chalmers University of Technology, Göteborg, Sweden, 2000.
2. Niemand, L.: *Probabilistic Establishment of Vehicle Fatigue Test Requirements*. Master of Engineering Thesis, University of Pretoria, Pretoria, 1996.
3. Thomas, J.J., Perroud, G., Bignonnet, A., Monnet, D.: Fatigue Design and Reliability in the Automotive Industry. In Marquis, G. Solin, J. (editors), *Fatigue Design and Reliability, ESIS Publication 23*. Oxford, UK: Elsevier Science, pp.1-12, 1999.
4. Grubisic, V., Fischer, G.: Methodology for Effective Design Evaluation and Durability Approval of Car Suspension Components. *SAE Technical Paper 970094*, 1997.
5. Fischer, G.: Design and Quality Assurance of Vehicle Components based on the Usage Related Stress Analysis. *XXIX Convegno Nazionale dell'Associazione Italiana per l'Analisi delle Solleciatazioni*, Lucca, 6-9 Sept. 2000.
6. Aurell J., Edlund S.: Operating Severity Distribution a Base for Vehicle Optimization, *11th IAVSD-Symposium on the Dynamics of Vehicles on Roads and Tracks*, Kingston, Canada, 1989.
7. Aurell J., Edlund S.: Prediction of Vibration Environment in Real Operations Described by Q-distributions, *14th IAVSD - Symposium on the Dynamics of Vehicles on Roads and Tracks*, Ann Arbor, USA, 1995.
8. Öijer, F., Edlund S.: Complete Vehicle Durability Assessments Using Discrete Sets of Random Roads and Transient Obstacles Based on Q-distributions, *17th IAVSD - Symposium on the Dynamics of Vehicles on Roads and Tracks*, Lyngby, Denmark, 2001.
9. Vägverket: Vägutformning-94 version S-1, del 6 Linjeföring. *Vägverket Publikation 1994-52*, Borlänge, 1994. (In Swedish).

Parameterisation of Lateral Fatigue Loads on Vehicles

Magnus Karlsson

Volvo Truck Corporation and
Department of Mathematical Statistics,
Chalmers University of Technology, SE-41296 Göteborg, Sweden

Abstract

A way of describing lateral acceleration for fatigue calculations is discussed. The purpose of the model is to parameterise the different sources of the fatigue load, such as the operating environment and the influence of the driver. The measured lateral acceleration is modelled with an approximative curvature, and the average speed explaining centripetal acceleration in the curve. The difference between the model and the observed lateral acceleration (the residual) is also studied. A way of extracting the curvature is presented and suitable statistical distributions for the curvature in city driving as well as driving on highways and secondary roads are suggested. A model for the relation between the curvature and the chosen speed is investigated. The acceleration residual is modelled by a transformed normal process. For the model of the centripetal acceleration an explicit expression for the expected cumulative fatigue damage using rainflow cycles is given, and expressions for the range spectrum is shown. For the residual an upper bound for the expected damage is shown. Comparison between the modelled loads and observed loads are made in terms of cumulative fatigue damage and range spectra. The influence of different drivers and markets are discussed.

1. Introduction

The truck industry is increasingly characterised by specialisation and customerisation. This means that the vehicle's specification and equipment must be tailored to suit each particular transport mission. The main focus is to optimise the performance to give the customer optimal transport efficiency, that is to maximise the productivity at the same time as the product cost is kept as low as possible.

The demands on transport efficiency (loading capacity, fuel economy etc.) and environmental friendliness have thus created a trend in vehicle development towards lightweight constructions. However, when using lightweight constructions it is necessary to make sure that the demands on reliability and durability are maintained, especially since component failures may cause loss of performance [1]. One of the major reasons for structural component failure is fatigue; therefore it is of great necessity to be able to predict what kind of loads the vehicle will experience during its intended life.

This task contains many difficulties. First of all the strength of the components varies due to variation in process and production, and secondly, and perhaps more importantly, there is a great variation in the loads depending on the application, the operating environment, the driver's behaviour and the vehicle specification. Due to insufficient knowledge about the loading conditions, the strength of components is often exaggerated through high safety factors. Many of these unnecessarily strong constructions can be avoided with a better understanding of the fatigue load in the real operating environment.

The natural way to acquire information about the service loading is to make field measurements of forces, strains etc. However, it is a troublesome and expensive task, especially since there is great variation in different customers' way of using their vehicles. Traditionally the field measurements have, via some cycle counting algorithm, been transformed into loading spectra. The loading spectra are then parameterised in different ways often using statistical techniques, and from this parameterisation, conclusions about the fatigue life are drawn. (See [2,3]) Klemenc and Fajdiga [2] treat the cycles as random variables, and try to find suitable distributions explaining the behaviour of the cycles, while Grubisic and Fischer [3] claim that they know the general shape of the loading spectra for different types of excitation mechanisms and therefore their focus is on trying to find out the maximum load and the number of cycles which give the spectra.

There are, however, some problems with the commonly used methods. Since the field measurements have seldom been considered long enough they have often been performed in such a way that the driver has been driving at high speed over a bad road stretch. However, it is very unclear just how damaging this driver and road is, and how this relates to the actual usage of a truck. In the same way the durability test tracks have been constructed to replicate the worst-case loading conditions that have been found during field measurements. [4]

There are other suggestions on how to get the fatigue load design specifications more related to the actual customer environment, for instance by using questionnaire surveys, (see [4, 5, 6].), but these methods do not appear to be reliable enough, since they are based on a subjective judgement and the results are very sensitive to the type of questions asked.

Another problem arises when trying to use the measured fatigue load at early design stages. Since the construction of prototypes when testing new components is a very expensive and time-consuming task, computer models have become very important for testing at early stages in the designing of new components. [7] However, the loads that the vehicle will experience during the measurements will to a great extent be determined by the vehicle design, and therefore there is little point in using measurements from old components, when trying to understand the loads for new components. Consequently, it would be interesting having some sort of vehicle independent description of the loads.

Rather than attempting to describe the loads as such, we here use a method based on the question: *What causes the loads?* As pointed out above there are several different factors: *the operating environment*, that is the roads that the truck will be driven on, *the driver's behaviour*, such as speed changes and manoeuvring and *the transport mission*. Also the technical design of the truck will affect the loads, i.e. *the vehicle specification*. If one could separate these different factors and describe them one by one and understand how they interact, much would be gained since the description of the operating environment would hold for any truck, the same would probably be true to a great extent for the driver's behaviour. (A reckless driver is most likely reckless no matter what truck he is driving.) It could therefore be of great interest to get a parameterisation of the actual road conditions and then model how drivers behave on these roads. Through such a description it would be possible to recreate the loads, and

the increased understanding of the origins of the loads would lead to a better understanding of the markets and applications.

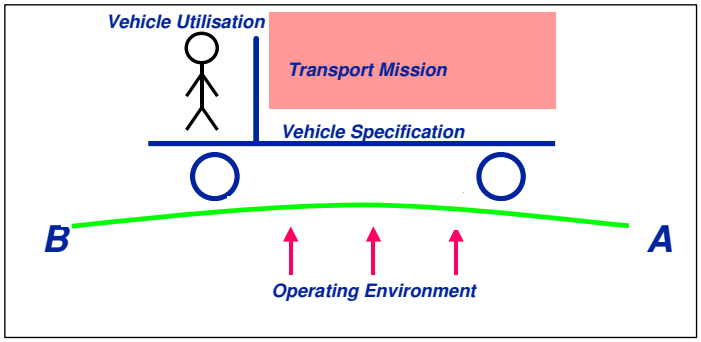

Figure 1. Different sources of fatigue load.

The loads that the truck will experience on the road come from different excitation mechanisms; some will, for instance, be due to an uneven road surface while others are due to the curvature. It appears to be current practice to separate different kinds of excitation mechanisms from each other, see [3,8,9]. Volvo's approach to the problem has been to describe different kinds of vehicle independent parameters called Global Truck Application (or simply GTA) parameters. (See [7].) The aim of the GTA concept is to secure that the vehicles are specified, developed and sold with the same view of usage in mind.

The most important excitation mechanisms should be those coming from driving into potholes and bumps, road vibration, curvature, braking and accelerations. The potholes and bumps together with the road vibration is in GTA described as road condition and has been considered in a series of articles by Volvo, see [10,11,12,13].

This work focuses on lateral loads. In order to describe lateral loads in terms of load origins, it is necessary to be able to describe the road, i.e. the curvature, the driver's behaviour, i.e. the speed and the driver's response to other factors than the road, as well as the vehicle's behaviour.

The paper is outlined in the following way. In section 2, the parametric model for the lateral acceleration is described. In section 3, the procedure for estimating the curvature is given, and the variability of the curvature is suggested to follow a lognormal-like distribution. In section 4, the average speed in a curve is modelled depending on the estimated curvature of the particular curve. In section 5, the models for the curvature and the speed are brought together to explain parts of the lateral acceleration. The remaining part is suggested to follow a transformed normal process. This gives us a parametric model of the lateral acceleration, in terms of road curvature, speed and response to other characteristics than the road. In section 6, the expected cumulative fatigue damage for the modelled load is devised, and an expression for range spectrum

is shown. For the residual an upper bound for the expected damage is found. In section 7, results are presented in terms of range spectra for measured loads and according to the expressions in section 6. Tables of damage for the observed loads are also shown together with damage found according to the expressions in section 6. In section 8, the results are discussed and some conclusions drawn. Finally, in section 9, some future work is suggested.

2. Model summary

The aim of this work is to parameterise the lateral loads according to the ideas outlined above, i.e. separating the different load origins, describing them one by one, and understanding their interaction. On this description, a way to classify measured load signals depending on their fatigue damage can be devised. The measurements used are lateral acceleration and velocity.

The cumulative fatigue damage depends on which stress the vehicle experiences. Since the stress at any point is directly proportional to the applied force, it is also proportional to the acceleration at that point. This means that the only distinction between calculating the damage from the acceleration rather than the stress should be a factor that can be determined by the proportionality. We can, thus concentrate on describing the acceleration. The lateral acceleration is found by multiplying measured signals of the velocity and the yaw rate. The proportionality constants will be different from point to point on the vehicle, but the key issue here is to be able to compare damage found from the loads in one measurement to that in another. Consequently, the method will not lead to a number that explains exactly how damaging the measured loads are but will rather make it possible to compare different measurements to each other.

The aim here is to describe the lateral acceleration using the concept explained above, that is separating the different load origins, describing them one by one, and understanding their interaction. According to this concept a parametric model for the lateral acceleration has to contain a description of the curvature of the road and a model for the velocity at which the driver chooses to driver through the curve. Ideally this would be enough, since the lateral acceleration can be calculated using the equation for centripetal acceleration. However, since the driver might be affected by other factors, the vehicle dynamics might affect the acceleration, and since the road surface may also lead to lateral acceleration and there may be measurement errors, the model of the lateral acceleration is constructed in the following way:

I. A model for estimating the curvature of each curve is developed. The curvatures found are modelled statistically, given a distribution of the curvature of the measured road.
II. A relationship between the driver's choice of speed and the curvature is explained with a regression model.
III. The part of the measured acceleration, which cannot be described in terms of simple centripetal acceleration (which can be found from I. and II. above) is modelled with a transformed normal process.

The steps I-III give the following equation and figure:

$$a_{meas}(t) = a_{centripetal}(t) + a_{res}(t) = v^2(t)C(t) + a_{res}(t) \quad (1)$$

where C is the curvature, v is the average speed along each curve and a_{res} is the residual acceleration. We here assume that the function $v(t)$ is constant along the curve and $C(t)$ is constant along the top of the curve. See right part of Figure 2.

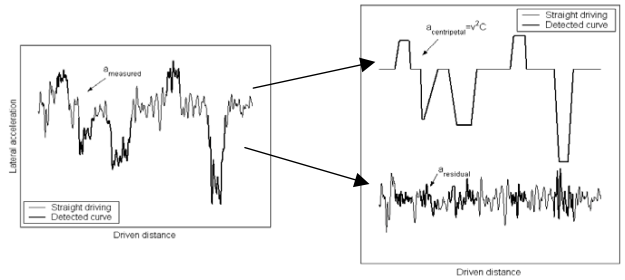

Figure 2. Separating the different parts of the acceleration.

The steps I-III above are then used to understand the cumulative fatigue damage, which the acceleration causes. Obviously (I) can be interpreted as the operating environment. (II) describes the driver's behaviour in terms of choice of speed. However, the effect of the driver can also be seen in (III), since part of this acceleration comes from the driver's response to other factors than the road. The issue is now to get a description of each of the three parts in the eq. (1) above, i.e. the curvature (C), the speed (v) and the residual (a_{res}) as functions of time or summarised in the form of distributions. These parts will, as was mentioned in the introduction, be described in section 3-5. In total there will be 9 parameters explaining the whole signal.

In the three steps (I-III) above a measurement can be described with a set of parameters. Since there is an interest in understanding how much damage the two parts of eq. (1) creates each, an approximation of the damage of the whole model is done in the following way:

$$D_{meas} \approx D_{trap} + D_{res} \quad (2)$$

where D_{meas} is the damage caused by the observed lateral load, D_{trap} is the damage caused by centripetal acceleration, i.e. the signal $C(t) \cdot v^2(t)$ in eq. (1). See also the right part of Figure 2), and D_{res} is the damage caused by the residual process, where consideration is also given to the interaction effect between the two signals. A motivation for this approach can be found in section 6.

3. The curvature model

When constructing a curve a crucial part is to make sure that vehicles driving through the curve will not experience too high lateral accelerations. In order to avoid this and to get a smooth ride through the curve it is therefore useful to have a constant curve radius over a longer time, say a couple of seconds. One way of modelling a curve would therefore be to think of it as having a constant radius over the entire curve. However if the curve is narrow, i.e. has a small radius, it is probably better to have an area at the beginning (and the end) of the curve where the radius is adapted to the part with a small constant radius. Thus it would be easier for a driver to adjust to the smaller radius. This concept can also be seen in road construction descriptions such as [14], but has also been used in models for velocity profile planning [15].

From a mathematical point of view it turns out that it is possible to model the curvature (here defined as the inverse of the radius at any point of the road) as following a trapezoid. (See Figure 3 and [16].)

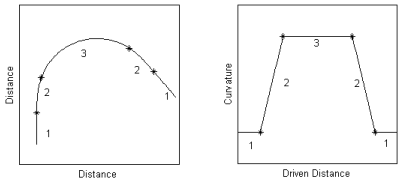

Figure 3. To the left: A straight part before entering the curve (1), an adaptation area where the radius decreases (2), and an area of constant radius (3). To the right: The curvature for the same curve.

The trapezoid, which describes the curvature, is here expressed with the following equation:

$$f(x) = \begin{cases} k_1 \cdot (x - (x_0 - L/2 - h/k_1)), & x_0 - L/2 - h/k_1 \le x < x_0 - L/2 \\ h, & x_0 - L/2 \le x < x_0 + L/2 \\ k_2 \cdot ((x_0 + L/2 + h/k_2) - x), & x_0 + L/2 \le x \le x_0 + L/2 + h/k_2 \end{cases} \quad (3)$$

where the different parameters can be seen in Figure 4 below:

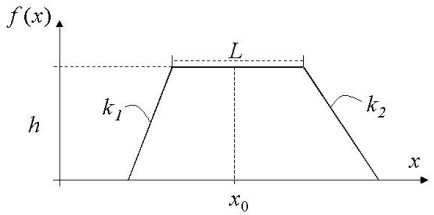

Figure 4. The mathematical model of the curvature as a trapezoid, where h is the height, L is the length of the top, x_0 is the driven distance of the middle of the trapezoid, and k_1 and k_2 are the slopes of the sides.

In [16] an algorithm for estimating the curvature using measurements of the yaw rate and the speed of a vehicle is described. Curves are detected using simple threshold criteria for some signals (speed, lateral acceleration and wheel angle), then for each detected curve a trapezoid is fitted to the signal corresponding to the curvature. Proving ground measurements, as well as video recordings from field measurement, were used to verify the algorithm.

Using this algorithm it is possible to estimate the curvature of each curve. A statistical distribution can then be fitted to the estimated maximal curvatures. It was suggested in [16] that the lognormal distribution might be a good distribution to fit to the data. However, from the result in [16] it was also clear that the data could not be described with a single distribution. The reason for this is that there are very different characteristics of the curves in a city compared to those in the countryside. Therefore, it would be reasonable to have one description for city driving and one for secondary roads and highways. To test this, a series of measurements performed in Brazil was used. The curves in the city stretch were separated from the rest, and the estimated maximal curvatures were fitted to different distributions.

The fact that there is a minimal turning radius sets a natural limit to the curvature distributions. Due to this limit no curvature can be higher than the inverse of the minimal turning radius. In order to find distributions for the curvature, it is therefore suitable to transform the maximal curvature in the following way:

$$Y_j = C_j^{-1} - r_{turn} \tag{4}$$

where C_j is the maximal curvature in curve j and r_{turn} stands for the minimal turning radius. It turns out that the lognormal distribution well describes the transformation (Y_j) of the curvature. However, as mentioned above, different distributions must be used for different kinds of roads. See Figure 5 below:

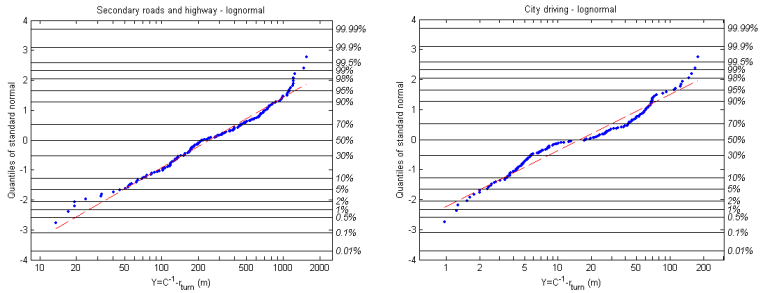

Figure 5. The transformed curvature appears to follow a lognormal distribution, for secondary roads and highway. A lognormal distribution could also be applied to curvature in city driving although the fit appears to be somewhat worse in this case.

In Figure 5, it is worth noticing that the scales of the x-axes in the two plots are very different. It can be seen that more than half of the curves on secondary roads and highways have a radius of more than 200m, while a majority of the curves in the city have a radius of less than 50m. The separation is hence reasonable, since it gives simpler forms for the distribution than a combined description would give.

The fact that it is possible to describe the variability in Y_j with lognormal distribution gives us the following probability density function for the maximal curvature, C_j:

$$f_{C_j}(c) = \frac{1}{\sqrt{2\pi\sigma_c^2}} \cdot \frac{1}{c(1 - r_{turn}c)} \cdot \exp\left(-\frac{1}{2} \frac{\left(\ln\left(\frac{1}{c} - r_{turn} \right) - \mu_c \right)^2}{\sigma_c^2} \right) \tag{5}$$

where the parameters μ_c and σ_c are the two parameters in the lognormal distribution for Y_j, i.e. $\log(Y_j) \in N(\mu_c, \sigma_c^2)$. We now have a statistical distribution describing the maximal curvature using 3 parameters.

4. The speed model

There are two different reasons why a speed model is necessary: there is a need to understand the driver's behaviour, and of course it is also necessary to model the speed to be able to relate the curvature to acceleration in order to be able to calculate the cumulative fatigue damage.

If a driver chooses to drive at the same speed through a narrow curve as a broad curve, the lateral acceleration will be greater in the narrow curve due to centripetal acceleration. In order to avoid this it is necessary for the driver to have some strategy when choosing the speed depending on the curvature. There are studies on modelling

the relationship between the radius of a curve and the speed at which the driver choose to drive through the curve, (see for instance [17]) but most such studies appear to focus on passenger cars. Three different models were tried out here, according to the following:

$$v_j = ae^{-bC_j+\varepsilon_j} \qquad \text{model (1)}$$

$$v_j = aC_j^{-b}\cdot e^{\varepsilon_j} \qquad \text{model (2)}$$

$$v_j = \begin{cases} aC_j^{-b}\cdot e^{\varepsilon_j}, & C_j \geq C_{\lim} \\ aC_{\lim}^{-b}\cdot e^{\varepsilon_j}, & C_j < C_{\lim} \end{cases} \qquad \text{model (3)}$$

Here v_j is the average speed in curve j taken over the part of the curve, where the maximal curvature can be found. (See Figure 2.) The maximum curvature found in curve j is denoted by C_j. We have seen above that the curvature can be found as $C_j = 1/r_j$. The entities a and b are the regression parameters and ε_j is a random deviation from the linear model, which is assumed to have zero mean and constant variance σ_ε^2 for all curves. The deviations $\{\varepsilon_j\}$ are assumed to be independent. Here $C_{\lim}$ is the smallest curvature for which the driver has to adopt the speed.

Model (1) above assumes an exponential relationship between the speed and the curvature, while model (2) assumes a power relationship and model (3) assumes a power relationship along with a cut-off radius, above which the speed is a constant times a stochastic deviation. The physical explanation for the last model is that it is reasonable to assume that for broad curves (low curvature) other effects rather than the curvature will determine the driver's choice of speed, such as the surrounding traffic, speed limits and the engine momentum. Below some curvature $C_{\lim}$, the driver is therefore no longer assumed to adopt the speed to the curve, but rather to other phenomena. This parameter can simply be found through the mean velocity during the straights as $C_{\lim} = (a/v_{\lim})^{1/b}$, where the mean velocity $v_{\lim}$ is the mean velocity that the driver uses when he is not adapting to the curvature of the road.

As the parameters a and b in the model depend on the driver they are in a sense random. The same holds for $C_{\lim}$, which is estimated from the measurement, but will mainly depend on the speed limits and traffic situation of the particular market.

The parameters a and b in the two first models can be found using simple linear regression. In the third model the standard linear regression no longer applies. However, a maximum likelihood technique can still be used to estimate the parameters of the model. The likelihood function for model (3) can be written as

$$L(a,b,\sigma_\varepsilon^2) = \prod_{i=1}^{n}\left(\frac{1}{\sqrt{2\pi\sigma_\varepsilon^2}} e^{\left(\frac{(\ln v_j - \ln a + b\ln C_j)^2}{2\sigma_\varepsilon^2}\right)} I_{(C_j < C_{\lim})} + \frac{1}{\sqrt{2\pi\sigma_\varepsilon^2}} e^{\left(\frac{(\ln v_j - \ln a + b\ln C_{\lim})^2}{2\sigma_\varepsilon^2}\right)} I_{(C_j \geq C_{\lim})} \right) \qquad (6)$$

where $C_{\lim}$ is as above. Estimates for the parameters can be found by maximising the likelihood function, which in this case has to be done numerically.

The models were applied to a series of measurements from Brazilian roads. It turns out that the model (1) gives very poor fit, and can be excluded. The second and third models appear to give good and similar results, which is reasonable since they are very similar in structure. (The cut-off curvature only applies to a small number of the detected curves.) The variability of the deviations ε_i in the second and third models are well described by a normal distribution, and appear to give results with small influence of the radius. See figures below.

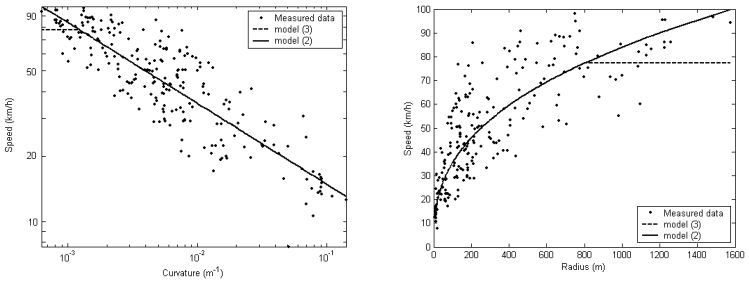

Figure 6. The speed models plotted together with measured data. To the left the curvature versus the average speed, showing what the actual relationship in log log scale looks like and to the right the radius (the inverse of the curvature) versus the speed in linear scale.

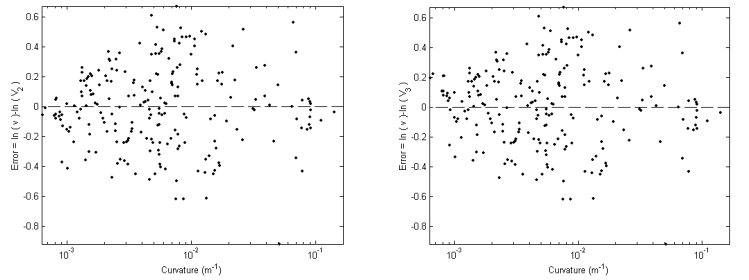

Figure 7. The errors plotted for model (2), to the left, and for model (3) to the right. The errors seem to have some influence from the curvature. There appear to be somewhat smaller errors when the curvature is small. The differences between the figures can be seen in the left parts.

The second model has the advantage of being simple. However, the physical interpretation of very broad curves is questionable. The model suggests that if the radius is large (i.e. the curvature is small) the speed should be large. Thus, in principal if the radius goes to infinity the average speed also has to go to infinity. It can also be noted from Figure 6 that according to model (2) the average speed at a curve of a radius of 1600m would be above 100km/h, which seems fairly unreasonable. It therefore seems like a good idea to choose model (3) as the one to use. Using model (3) we now have four parameters describing the relation between curvature and mean speed.

One way of creating a subtler model for the velocity given the radius would be to use the above model but to include such physical restrictions as speed limits and the limiting lateral acceleration for the vehicle to turn over.

5. Modelling the acceleration signal

Using the equation for centripetal acceleration we can find the part of the acceleration corresponding to the actual curvature from the curvature model and the speed relation in the following way:

$$a_{trap}(t) = \frac{v^2(t)}{r(t)} = v^2(t) \cdot C_{trap}(t), \tag{7}$$

where $v(t)$ is constant over each curve and equal to the average speed along the part of the curve, where the maximal curvature is found. The measured acceleration can be seen as determined by the acceleration from the curvature and a residual on top of that, or as two random processes corresponding to the curvature and the residual, which are modelled as being independent of each other. The residual part mainly corresponds to the driver's response to other factors than the road, the effect of the vehicle and the unevenness of the road. It will be denoted a_{res}. The additive relation can be seen in the following way:

$$a_{meas}(t) = a_{trap}(t) + a_{res}(t) = v^2(t) C_{trap}(t) + a_{res}(t) \tag{8}$$

We will from now on use model (3) for the speed presented above. The curvature and the speed, as described above, can now be combined to model the trapezoidal part of the acceleration, that is the maximum centripetal acceleration in any curve j is:

$$a_{trap,j} = v_j^2 C_j = \begin{cases} a^2 C_j^{1-2b} e^{2\varepsilon_j}, & C_j \geq C_{\lim} \\ a^2 C_{\lim}^{-2b} C_j e^{2\varepsilon_j}, & C_j < C_{\lim} \end{cases} \tag{9}$$

This expression relates to the expressions for $a_{trap}(t)$, $C_{trap}(t)$ and $v(t)$ in such a way that $a_{trap}(t) = a_{trap,j}$, $C_{trap}(t) = C_j$, and $v(t) = v_j$ if t is within the interval over curve nr j where maximal curvature C_j is found. The remaining part of the acceleration that cannot be described with the trapezoidal part can be thought of as a random process. It

turns out that it is reasonable to model this residual acceleration as a transformation of a normal process in the following way:

$$X(t) = sign(a_{res}(t)) \cdot \sqrt{a_{res}(t)} \in N(0, \sigma_{res}^2) \tag{10}$$

See Figure 8 below. This implies that $a_{res}(t) = sign(X(t)) \cdot X^2(t)$, where $X(t) \in N(0, \sigma_{res}^2)$, and σ_{res}^2 is the variance of $X(t)$. Unfortunately, there is no physical explanation for this expression, but it could still be argued from Figure 8 below that the fit looks very good for the vast majority of the values, where in total roughly $2 \cdot 10^6$ are considered.

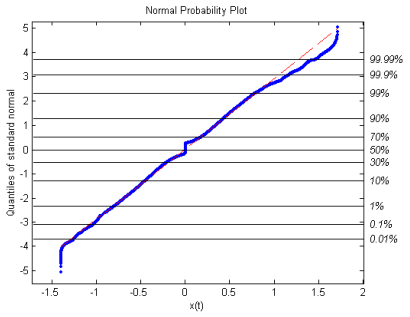

Figure 8. The transformation of the residual appears to follow a normal distribution.

It remains to be seen if the assumption of independence between the residual and the centripetal acceleration holds. It turns out that the variance estimated from the curves is only 8% greater than the variance of the straight parts, and the sample correlation between the sample variance of the residual and the centripetal acceleration over the curves is –0.03. From these results it appears to be justified to assume that the residual is independent of the centripetal acceleration. Hence, the variance is from now on assumed to be constant over the entire signal.

The idea of the division of the acceleration into two parts is that the lateral acceleration can be seen as a two-folded signal, one part coming from the construction of the road and one part from the way the particular driver uses the vehicle.

We now have a parameterisation of the lateral acceleration into a small number of parameters that describe the measurement. In order for such a parameterisation to be useful it must be possible to calculate the fatigue damage from the parameterisation, as we need to be able to compare the damage that different markets cause.

6. The cumulative fatigue damage for curvature

6.1. A damage approximation

The damage caused by a load is often calculated using the rainflow count algorithm and damage rules such as the Palmgren-Miner rule. (See appendix A1.) As can be seen from the Palmgren-Miner rule, the cumulative fatigue damage, which a component will experience, can be determined from the stress applied to the particular component. The stress is directly proportional to the force, and therefore also to the acceleration. According to the trapezoid model above we can divide the measured acceleration into two parts, one corresponding to the fitted trapezoids, and one corresponding to the residual, see eq. (8).

A natural question to ask is: How much of the damage can be explained by the road and the choice of speed, and to what extent does the residual affect the damage? If we just calculated the acceleration corresponding to the trapezoid and add that to the damage from the acceleration from the residual, according to eq. (11) below, there would be an error;

$$D(a_{meas}(\cdot)) \approx D(a_{trap}(\cdot)) + D(a_{res}(\cdot)) \tag{11}$$

where $D(x(\cdot))$ is the damage caused by the process $\{x(t)\}$. The problem with this method is twofold. First of all cumulative damage when calculated from rainflow cycles is not a linear function not even for $\beta = 1$, where β is the slope of the Wöhler-curve (see appendix A1), so this addition is simply wrong. However, in the special case that we have here, where we have two processes that vary with very different derivatives over the signal, see Figure 9 below, the approximation works well.

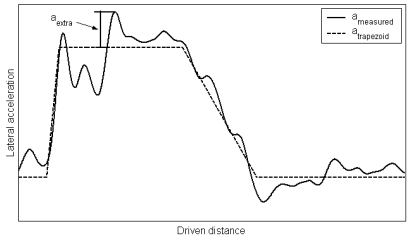

Figure 9. The derivatives for the residual is much larger than the derivatives for the centripetal acceleration on the straight parts and where the curvature is constant, while the opposite is true on the part at the beginning and the end of the curves. The largest residual over the curve is denoted a_{extra}.

The reason for this is the following: in the straight parts of the road and in the parts with a constant curvature the derivative of the residual is obviously much greater than the derivative for the centripetal acceleration, which is zero. On the other hand, through the parts of the curve, where the curvature increases, the centripetal acceleration has a much greater derivative. For this reason the assumption that is made of linearity will work fairly well, despite the approximation.

The second problem with eq. (11) is that it does not take into consideration the fact that the largest cycles of the actual measured signal will be due to the interaction between the trapezoids and the peaks of the residual acceleration. (See Figure 9.) A way of correcting for this error is to model the maximum of the residual over a curve and then add that to the curvature part (that is a_{trap}). Thus we can use the acceleration from the trapezoid model added with the extra loads coming from the maxima of the residual over each curve (here denoted a_{extra}), and let this correspond to the largest cycles. We can, however, still see the effect of the trapezoid acceleration with the following rearrangement:

$$D_{meas} \approx D_{trap} + D_{res} \tag{12}$$

where

$$D_{meas} = D(a_{meas}(\cdot)), \quad D_{trap} = D(a_{trap}(\cdot)) \tag{13}$$

and

$$D_{res} = D(a_{res}(\cdot)) + \left[D(\hat{a}_{trap}(\cdot)) - D(a_{trap}(\cdot))\right] \tag{14}$$

where

$$\hat{a}_{trap}(t) = a_{trap}(t) + a_{extra}(t). \tag{15}$$

The last term in eq. (14), i.e. $\left[D(\hat{a}_{trap}(\cdot)) - D(a_{trap}(\cdot))\right]$, takes care of the problem of missing the largest loads over the curve. This explains what effect the interaction between the trapezoid and the residual has. The entity a_{extra} is, as mentioned above, the maximum of the residual over each curve.

This entity a_{extra} is fixed for each curve, and thus with the addition in eq. (15) we get that over the whole curve $\hat{a}_{trap}(t)$ increases with the value a_{extra}. However, with the assumption that damage is a rate independent process the only important part is the maxima over each curve, and thus the addition in eq. (15) works. This is true no matter whether we look at the centripetal acceleration a_{trap} or include the maximum of the residual, i.e. look at $\hat{a}_{trap}$. It should be noted that when there are two curves in the same direction, a similar extra term to a_{extra} could also be included for the largest value in the opposite direction to the curves through the straight part in between them, but this is not included in the model.

The overshot a_{extra} is here assumed to be independent of the centripetal acceleration a_{trap}. This can be justified by the fact that in the measurements used here the correlation between these two variables was found to be less than 0.8%, i.e. it seems as if the maximum residual acceleration over each curve is independent of the centripetal acceleration governed by the curvature of that curve. From the measurements, it turns out that the variability of the extra loads is well described by the exponential distribution. See Figure 10 below.

The exponential distribution will be used to model a_{extra} from here on. Knowing the distributions for a_{trap} and a_{extra} it is also possible to find the distribution for $\hat{a}_{trap}$.

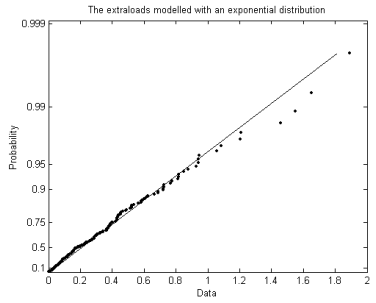

Figure 10. Extra loads plotted on an exponential distribution paper.

The method of dividing the damage into the two classes mentioned above can be illustrated by Figure 11, showing the range spectrum for the measured lateral acceleration a_{meas}, along with the sum of the range spectra for the measured maximal lateral accelerations over the curves and the residual acceleration. It should be noted that this summation is done in the x-direction of Figure 11. At each range, it can be seen that the sum of number of cycles from the residual and the trapezoids with the extra loads is slightly greater than the number of cycles for the measured signal.

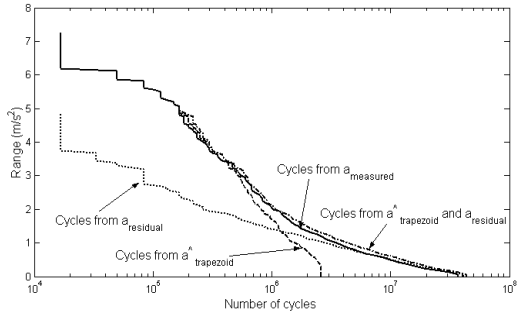

Figure 11. The range spectrum for the trapezoids with the extra loads and the range spectrum for the residual are shown. Adding the cycles from the two yields a result very close to the cycles from the original measurements, justifying the approximation in eq. (12).

As can be seen in the figure the combined ranges are very close to the measured ones. It follows that the cumulative fatigue damage for the two parts summed together also should be close to the damage coming from the measurement. It is also worth noticing in Figure 11 that the residual actually contributes quite a lot to the range spectrum and

thus the damage from this part cannot be ignored. In the particular measurement depicted in Figure 11, $D(a_{res}(\cdot))$ explains more than 20% of D_{meas}.

6.2. Rainflow cycles

As already mentioned the most important measure that we are working with is the cumulative fatigue damage. In order to verify that the model describes the loads it is therefore necessary to investigate how damaging (in terms of cumulative fatigue damage) the modelled loads are.

Over the years various methods of extracting fatigue relevant data from random load-time histories have been developed. One way of dealing with this problem is to form equivalent load cycles and then use damage accumulation methods, such as the Palmgren-Miner rule [18, 19]. The most common counting methods are the range-pair counting method, the peak counting method, the level crossing counting method and the rainflow counting method. The method that has shown best results is the rainflow counting method. (See for instance [20].) The rainflow counting method was introduced by Endo 1967 in a series of papers by Endo et al. [21, 22] and Matsuishi and Endo [23]. It has become the most commonly used counting method in engineering. The rainflow cycle algorithm was designed to catch both slow and fast variations of the loading by forming cycles that pair high maxima with low minima even if they are separated by intermediate extremes. The way of constructing the cycles is based on counting hysteresis cycles for the load in the stress-strain plane. One possible definition is the following, first presented by Rychlik [24]:

Definition 1:

From the *i*:th local maximum (value M_k) one looks at the lowest values in forward and backward directions between M_k and the nearest point in the forward direction at which the load exceeds (or equals) M_k and the nearest point in the backward direction at which the load exceeds M_k. The larger (less negative) of those two values, denoted by m_k^{rfc}, is the rainflow minimum paired with M_k, i.e. m_k^{rfc} is the least drop before reaching the value M_k again on either side. Thus the *i*:th rainflow pair is $\left(m_k^{rfc}, M_k\right)$ and the rainflow amplitude is $H_k^{rfc} = M_k - m_k^{rfc}$.

This definition is probably best understood from a figure:

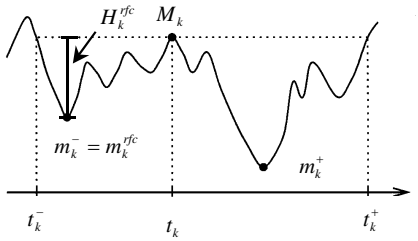

Figure 12. The definition of the rainflow cycle. The rainflow cycle is denoted H_k^{rfc}

We have already seen that a load can be considered a sequence of cycles, which are formed by a combination of local maxima and minima. The cycles can be constructed using the rainflow counting method. The aim now is to find the expected damage for the different parts in eq. (16) and (17) trapezoid acceleration signal $a_{trap}(\cdot)$, the trapezoid acceleration when the extra loads are considered $\hat{a}_{trap}(\cdot)$ as well as for the residual $a_{res}(\cdot)$. The distribution for the trapezoid acceleration is now useful. As we will see it provides a possibility to make exact calculations of the expected damage and the range spectrum for the cases when we consider $a_{trap}(\cdot)$ and $\hat{a}_{trap}(\cdot)$. For the more difficult $a_{res}(\cdot)$ an upper bound will be found.

6.3. Expected damage for the trapezoid acceleration

We can, from eq. (9) calculate the distribution of the amplitude of the trapezoid acceleration in each curve, using our knowledge of the distribution of the curvature and the errors. Since we also know the distribution of the extra loads, the distribution for $\hat{a}_{trap,i}$ in each curve i can also be calculated. Since we only need to consider the local maxima and minima the load, no matter whether we look at $a_{trap}(\cdot)$ or $\hat{a}_{trap}(\cdot)$, can now be described as a sequence of random variables $\{X_i\}$, where every second value is zero and the values in between are either positive or negative with probability $1/2$ each, and whose amplitude is decided according to the distribution of the trapezoid acceleration. This can be seen in the following way, that each X_i has the following distribution:

$$X_i \overset{D}{=} \begin{cases} 0, & \text{if } i = 0, 2, 4, \ldots \\ Z, & \text{with prob. } 1/2, \text{ if } i = 1, 3, 5, \ldots \\ -Z, & \text{with prob. } 1/2, \text{ if } i = 1, 3, 5, \ldots \end{cases} \tag{18}$$

where Z is distributed according to the distribution of the amplitude of the trapezoid acceleration, i.e. when not considering the extra loads we have that

$$Z \overset{D}{=} C_j \cdot v_j^2 = \begin{cases} a^2 C_j^{1-2b} e^{2\varepsilon_j}, & C_j \geq C_{\lim} \\ a^2 C_{\lim}^{-2b} C_j e^{2\varepsilon_j}, & C_j < C_{\lim} \end{cases} \tag{19}$$

and when also considering the extra loads $a_{extra,j}$ we get

$$Z \overset{D}{=} C_j \cdot v_j^2 + a_{extra,j} = \begin{cases} a^2 C_j^{1-2b} e^{2\varepsilon_j} + a_{extra,j}, & C_j \geq C_{\lim} \\ a^2 C_{\lim}^{-2b} C_j e^{2\varepsilon_j} + a_{extra,j}, & C_j < C_{\lim} \end{cases}. \tag{20}$$

Note in eq. (18) that the zeros are necessary to include since there are extremes, which have value zero. This is for instance the case when we have two curves in the same direction as can also be seen in Figure 13, where an example of a sequence is depicted, and we have a zero local maximum for $i = 4$.

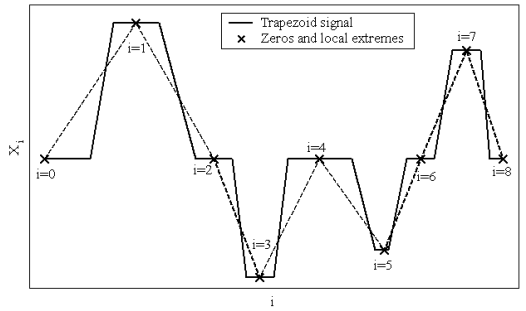

Figure 13. Trapezoid signal with marked zeros and local extreme values, which build up a sequence. The amplitude of each local extreme value is distributed according to the distribution of the amplitude of the trapezoid acceleration.

In the following, the amplitudes of the curves are assumed to be independent of each other, and that the direction of the curves are also independent. Assume now that we study a signal containing n curves. We can then study a sequence of $2n$ elements $(X_0, X_1, \ldots, X_{2n-1})$, where the element X_i can be found according to eq. (18).

Our wish is now to apply this sequence to the rainflow count method in order to find the cycles, and the expected damage. This can be done using a technique from Rychlik [24], but in order to do this we need the following definition:

Definition 2:

Let $L(t)$, $0 \leq t \leq T$, be a load and $\{(x,y)_{t_i}\}$ a cycle count. Let $N_T(u,v)$, $u \geq v$, denote a counting distribution of a cycle count $\{(x,y)_{t_i}\}$ defined as follows: $N_T(u,v) = \#\{(x,y)_{t_i}; t_i \leq T \text{ and } x > u \geq v > y\}$, i.e. the number of cycles with top higher than u and through lower than v. This can also be seen as interval up-crossings of the interval $[v,u]$.

Using this definition Rychlik [24] stated the following theorem:

Theorem 1 (Rychlik):

Consider a countable cycle count $\{(x,y)_{t_i}\}$ obtained from a load $L(t)$, $0 \le t \le T$, with a counting distribution $N_T(u,v)$ and let the damage caused by a cycle $(x,y)_{t_i}$, $f(x,y)$, be a twice continuously differentiable function such that $\partial^2 f(x,y)/\partial x \partial y \le 0$ for all $x \ge y$ and $f(x,x) = 0$. Then the total damage $D(T)$ is finite and given by

$$D(T) = -\iint_{u \ge v} N_T(u,v) \frac{\partial^2 f(u,v)}{\partial u \partial v} du dv - \int_{-\infty}^{\infty} N_T(u,v) \frac{\partial f(u,v)}{\partial v}\Big|_{u=v} du \tag{21}$$

For a proof of Theorem 1, see [25]. We are here assuming that the damage for one cycle is given by eq. (A4), with $\beta > 2$. (See appendix A1.) This means that we get the following damage function:

$$f(u,v) = K(u-v)^{\beta} \tag{22}$$

Using eq. (22) in eq. (21) and simplifying leads to the following result in our case:

$$D(T) = K\beta(\beta-1)\iint_{u \ge v} N_T(u,v) \cdot (u-v)^{\beta-2} du dv \tag{23}$$

Now, we are mainly interested in the expected damage caused by the signal up to time T. Let $\mu_T(u,v) = \mathbf{E}[N_T(u,v)]$, i.e. the expected number of up-crossings of the interval $[v,u]$ for the sequence until time T. Then, taking the expected value of eq. (23) leads to

$$\mathbf{E}[D(T)] = K\beta(\beta-1)\iint_{u \ge v} \mu_T(u,v) \cdot (u-v)^{\beta-2} du dv \tag{24}$$

where K and β are the constants in the Wöhler curve according to eq. (A1) in appendix A1. In order to be able to find the expected damage in our particular case we thus need to find $\mu_T(u,v)$, for $u \ge v$.

Let us now consider the sequence of length $2n$, where we have n curves, where the different values in the sequence are found according to eq. (18), and study three different cases for $\mu_T(u,v)$.

First assume that $0 < v \le u$. Since all local minima in our sequence will be ≤ 0, we can conclude that all cycles that manage to exceed u will have started from a value less than the positive v. The maximum values for the sequence (see Figure 13) can either be positive lateral acceleration or zero lateral acceleration. At all odd indexes, the probability of having a positive lateral acceleration, i.e. having $X_i > 0$ is $1/2$. Hence with a sequence of length $2n$ the average number of positive maximum values of the sequence is $n/2$. Finally, the probability for a curve with positive lateral acceleration to

exceed u can simply be found as $\mathbf{P}(Z > u)$. Combining this lead to the following expression for $\mu_{2n}(u,v)$ for the case when $0 < v \le u$:

$$\mu_{2n}(u,v) = \frac{n}{2} \cdot \mathbf{P}(Z > u) \tag{25}$$

Next consider the case when $v \le u < 0$. For our sequence all local maxima will be ≥ 0, we can conclude that all cycles that start from a value below v will always exceed the negative u. With the same reasoning as above it can be concluded that the average number of negative minima over the sequence must be $n/2$. The probability of having a curve with negative lateral acceleration less than v is $\mathbf{P}(-Z < v) = \mathbf{P}(Z > -v)$. Thus, for the case when $v \le u < 0$ we get

$$\mu_{2n}(u,v) = \frac{n}{2} \cdot \mathbf{P}(Z > -v) \tag{26}$$

The last case that we need to consider, which is the most difficult is when $v \le 0 \le u$. It can be shown, see appendix A.2, that this case leads to

$$\mu_{2n}(u,v) = \frac{n}{2} \cdot \frac{\mathbf{P}(Z > u) \cdot \mathbf{P}(Z > -v)}{\mathbf{P}(Z > u) + \mathbf{P}(Z > -v)} \tag{27}$$

To summarise we have now seen that the expected number of crossing of the interval $[v,u]$, where $u \ge v$ can be written as

$$\mu_{2n}(u,v) = \begin{cases} \dfrac{n}{2} \cdot \mathbf{P}(Z > u), & \text{if } u \ge v > 0 \\ \dfrac{n}{2} \cdot \dfrac{\mathbf{P}(Z > u) \cdot \mathbf{P}(Z > -v)}{\mathbf{P}(Z > u) + \mathbf{P}(Z > -v)}, & \text{if } u \ge 0 \ge v \\ \dfrac{n}{2} \cdot \mathbf{P}(Z > -v), & \text{if } 0 > u \ge v \end{cases} \tag{28}$$

This expression can now be applied to eq. (24). First, notice the symmetry between the two cases $0 < v \le u$ and $v \le u < 0$, and then since for a random variable such that $Z > 0$ we have that $\int_0^{\infty} \beta \cdot u^{\beta-1} \cdot \mathbf{P}(Z > u) du = \mathbf{E}[Z^{\beta}]$. With a few simplifications we can then state the following theorem:

Theorem 2:

For the assumptions made above, and a sequence of length $2n$, we get the following expected damage:

$$\mathbf{E}\left[D(2n)\right] = K \cdot \beta \cdot n \cdot \mathbf{E}\left[Z^{\beta}\right] + \frac{K \cdot n \cdot \beta \cdot (\beta - 1)}{2} \int_{u=0}^{\infty} \int_{v=-\infty}^{0} \frac{\mathbf{P}(Z > u) \cdot \mathbf{P}(Z > -v)}{\mathbf{P}(Z > u) + \mathbf{P}(Z > -v)} \cdot (u - v)^{\beta - 2} \, dv du \qquad (29)$$

Eq. (29) can now be evaluated numerically for a particular measurement in order to find the expected damage for the set of parameters of that measurement.

We have not included any dependence for the direction of two consecutive curves. It could of course be argued that it is more likely that a curve to the left will follow one to the right. There are several ways on which this could be incorporated. One possibility is to model the load as a Markov chain, and let a regime process determine the direction. Theoretical results for this could be found in Johannesson [26]. However, it might also be possible to find relatively simple expressions for the expected damage using the same kind of arguments as those used here.

6.4. Range spectrum evaluation

Apart from the damage it is also interesting to see results in terms of range spectra for the modelled loads and compare that with the results for measured loads. The plots of range spectra show in principle the number of cycles, whose ranges exceed a certain level plotted against that level. In the plots the number of cycles are found on the x-axis, and the level on the y-axis.

Let $\kappa(h)$ be the average number of cycles, whose ranges exceed level h. In our case we have three types of cycles, one with negative minima and positive maxima, another with negative minima and zero maxima and the last one having zero minima and positive maxima. By calculating the average number of cycles having a range exceeding the level h for each of these three cases and then add them together the following theorem can be shown that

Theorem 3:

For the assumptions made above and a sequence of length $2n$, we get the average number of cycles, whose ranges exceed h as:

$$\kappa(h) = n \cdot \frac{\mathbf{P}(Z > h)^2}{1 + \mathbf{P}(Z > h)} + \frac{n}{4} - n \cdot \int_{u=0}^{h} \int_{y=0}^{h-u} \frac{\mathbf{P}(Z > u) \cdot \mathbf{P}(Z > y) \cdot g_Z(u) \cdot g_Z(y)}{\left(\mathbf{P}(Z > u) + \mathbf{P}(Z > y)\right)^3} dy du \qquad (30)$$

where $g_Z(\cdot)$ is the probability density function for the distribution of trapezoid accelerations. For a proof of this result, please consult appendix A.3. An interesting observation of this formula is to let h tend to zero. The first term in $\kappa(h)$ then tends to $n/2$, while the last term vanishes and hence $\kappa(h)$ tends to $3n/4$, which is also the total number of rainflow cycles according to the model. (See appendix A.3.)

Through the results in sections 6.3 and 6.4 we now have a possibility to get the expected damage and the range spectrum for the trapezoid acceleration, and it is also possible to do the same calculations for the trapezoid acceleration when considering the extra loads, with the only change that the distribution for the accelerations becomes somewhat more complicated.

6.5. An upper bound for the expected damage from the residual

As part of the acceleration is described by a residual, (see eq. (1) above) there also has to be a description of how to get the damage for this signal, i.e. the $D(a_{residual}(\cdot))$. That the residual actually is quite important for the total damage can be seen from Figure 11, which shows that although the residual gives only few very high cycles it still makes up a considerable part of the range spectrum.

It is in general difficult to find the expected damage from a non-Gaussian random process. For Gaussian load cases there are some results such as [25], and there are also some approximations for more general cases such as in [27]. However, as mentioned above (see eq. (10)) the residual can be seen as a transformation of a Gaussian process. For such a transformation an upper bound can be found according to Rychlik [28]. For the particular transformation here we get that the following corollary shows the upper bound for the damage intensity:

Corollary:

If a random process $W(t)$ can be modelled as a transformed normal process with the following transformation: $W(t) = sign(X(t)) \cdot X^2(t)$, where $X(t) \in N(0, \sigma_{res}^2)$, then an upper bound for the damage intensity that the process causes can be seen as

$$d_W \le \nu \cdot 2^{2\beta} \cdot K \cdot \sigma_{res}^{2\beta} \cdot \Gamma(\beta + 1) \qquad (31)$$

where d_W is the damage intensity of the process $W(\cdot)$, ν is the intensity of zero-crossings, β is the slope in the Wöhler curve, K is the maximum load in the Wöhler curve (see appendix A1), σ_{res}^2 is the variance of $X(t)$ and $\Gamma(\cdot)$ is the gamma-function.

This corollary now indicates a simple way of getting an upper bound for the damage from the residual process, where we only need to estimate ν and σ_{res}^2 from the measurements. In the estimates of the damage caused by the residual acceleration this method will be used. For a proof of the corollary, see appendix A.4. It could be argued that it is necessary to consider that we have removed a number of the cycles caused by the residual since we have used one maximum of the residual for each curve, and thus we should decrease the intensity ν, but the total number of cycles for the residual is much larger than the amount of curves, roughly 50 times, and hence this effect is negligible.

7. Results

A series of measurements performed in Brazil and Germany were used to compare the modelled load with the actual measured ones. The parameters for the curvature, speed, residual and extra load were estimated from the measurements. From these it is then possible to find an approximation for the damage and range spectrum according to the ideas in section 6. The results can then be compared with the range spectra and damage directly estimated from the measurements.

Three of the measurements used here, were performed on the same stretches of roads in Brazil. These measurements are denoted measurement 1-3. The measurement denoted Brazil comes from a transport of sand on secondary roads in Brazil. The measurement denoted Germany comes from a highway in the Eastern parts of Germany.

7.1. Range spectra comparison

In the figures over range spectra below, the range spectra for the actual measurements are plotted together with the range spectra from the model using the estimated parameters. (The range spectra for the model have a smoother shape, and will also allow for greater ranges.)

In Figure 14, range spectra, on the basis of the trapezoid acceleration (a_{trap}) only, over each measurement can be seen. From the measurements the trapezoid acceleration was found, and the range spectrum was calculated from this signal. Then the parameters in the curvature and the speed model were estimated and from these estimated parameters (2 for the curvature and 4 for the speed model) the range spectrum for the model was calculated. The three different measurements used here are the measurements 1-3, which were performed on the same stretches of roads, but with three different drivers. For this reason, it can be seen that the total number of cycles (x-axis) are very close, while the effect of the driver can be seen in the way that driver 1 generally chooses a higher lateral acceleration than driver 3, while the most careful driver is driver 2. This is obviously also reflected in the results for the fitted models.

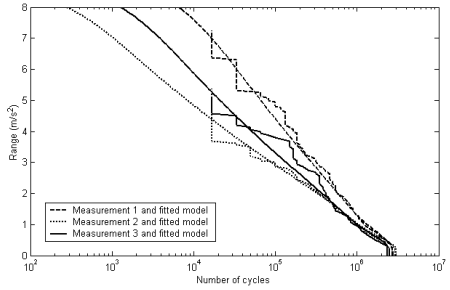

Figure 14. Range spectra for the trapezoid acceleration for three different measurements on the same road using different drivers.

In Figure 15, range spectra on the basis of the maximum acceleration over each curve can be seen. This corresponds to trapezoid acceleration when the extra loads are

considered (i.e. $\hat{a}_{trap}$). The three different measurements again refer to the three measurements on the same road using different drivers. As the only difference from Figure 14 is the inclusion of the extra loads, the difference is rather small, and we can once again see that the driver in Measurement 1 generally chooses the highest lateral acceleration and that the fitted models (the smoother curves) work well.

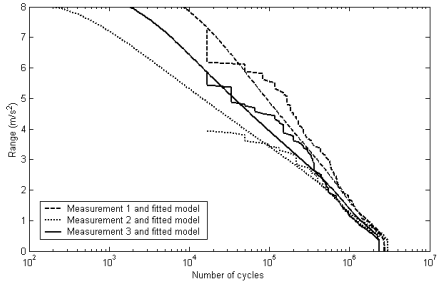

Figure 15. Range spectra for the trapezoid acceleration together with the extra loads for three different measurements on the same road using different drivers.

In Figure 16, range spectra for the whole measurements can be seen. These range spectra are compared with the spectra when the cycles from the model for $\hat{a}_{trap}(\cdot)$ are considered together with the cycles from $a_{res}(\cdot)$. The cycles from the residual is here only the measured ones and are thus not modelled, but the purpose is to show how the result for a whole measurement would look. According to eq. (12) this should be roughly the same, which could also be seen in Figure 11. The results in Figure 16 once again come from the three measurements on the same road.

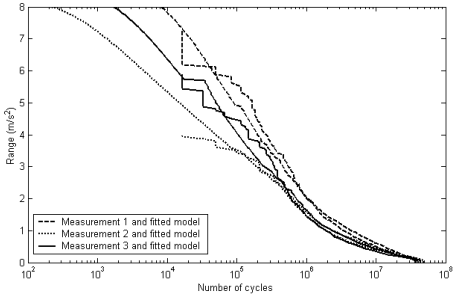

Figure 16. Range spectra for the model and the measured lateral acceleration.

Figure 17 shows the range spectra for the whole measurement for two different measurements performed in Germany and Brazil. The German measurement comes from a highway in the eastern parts of the country, and the Brazilian measurement is a transport of sand in the countryside. For reference purposes measurement 3 from Figure

16 is also included in Figure 17. It can be seen that the main difference is in the middle of the ranges (around $2m/s^2$).

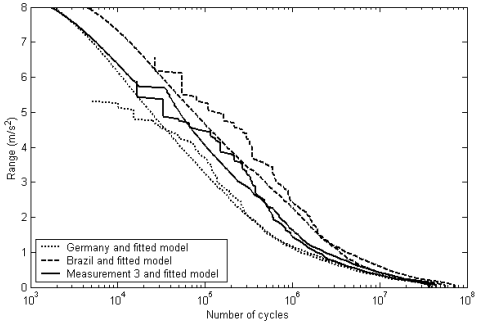

Figure 17. Range spectra for different measurements from Germany and Brazil.

7.2. Damage calculations for the residual approximation

The upper bound for the damage from the residual acceleration $D(a_{res}(\cdot))$, as can be seen in section 6.5, was calculated for the different measurements used above. The values are normalised by the damage for the observed loads in measurement 1.

		Meas. 1	**Meas. 2**	**Meas. 3**	**Brazil**	**Germany**
$\beta = 3$	Meas.	1	0.35	0.57	0.47	0.22
	Model	1.56	0.66	1.01	0.77	0.38
$\beta = 4$	Meas.	1	0.25	0.76	0.32	0.11
	Model	1.36	0.41	0.78	0.43	0.21

Table 1. The damage from the residual acceleration together with the upper bound for the different measurements. The calculations are made for two common slopes in the Wöhler curve.

It can be seen in Table 1 that although the model, which is an upper bound, yields larger damage than the measurement loads, the order of the measurements in terms of damage is preserved. (The loads in measurement 1 is the most damaging, followed by those in Meas. 3, Germany, Meas. 2, and the least damaging are the loads in the measurement denoted Brazil.)

7.3 Damage calculations for modelled and observed loads

In order to see how the model works for the entire measurements, the damage was calculated from the observed loads as well as using eq. (29) and (29). The results are presented in Table 2 below. All results are normalised by the damage caused by the measured lateral acceleration for the particular measurement. The entity D_{total} is defined as $D_{total} = D_{trap} + D_{res}$. Thus we can also see how well this approximation works in numbers.

$\beta = 3$		**Meas. 1**	**Meas. 2**	**Meas. 3**	**Brazil**	**Germany**
D_{trap}	*meas.*	*0.50*	*0.49*	*0.51*	*0.75*	*0.63*
	model	0.54	0.57	0.51	0.58	0.66
D_{res}	*meas.*	*0.60*	*0.61*	*0.64*	*0.31*	*0.38*
	model	0.67	1.20	0.97	0.51	0.63
D_{total}	*meas.*	*1.10*	*1.10*	*1.15*	*1.06*	*1.01*
	model	1.21	1.78	1.48	1.09	1.56
D_{meas}		*1*	*1*	*1*	*1*	*1*

Table 2. The damage from the different parts of the damage approximation in eq. (12). The measured signals are compared to the parameterised model. The calculations are made for $\beta = 3$ a common slope in the Wöhler curve. All results are normalised with the damage from their measured loads, respectively.

Table 3 is constructed to show how well the order of the damage for the measured loads is preserved when using the parameterised model rather than the observed loads.

$\beta = 3$	**Meas. 1**	**Meas. 2**	**Meas. 3**	**Brazil**	**Germany**
D_{meas}	1	0.29	0.49	1.17	0.25
D_{total}	1.21	0.52	0.72	1.27	0.39

Table 3. The damage from the damage approximation in eq. (12), compared to the damage from the measured loads. All values are normalised with the original damage of observed loads measurement 1. Once again the slope in the Wöhler curve is assumed to be $\beta = 3$.

Noteworthy in Table 3 is that the order of the measurements is preserved, though the fitted model gives too high damage in all cases. It is also interesting to notice that the damage caused by the residual load process for the Brazilian measurement is roughly half of the damage caused by the residual for measurement 1, but the total damage is actually greater for the loads in the Brazilian measurement.

8. Discussion and conclusion

As can be seen from the results the model appears to work rather well. The model provides a technique to determine the damage from one market and application to another. It is also possible to see the effects of the road in terms of the curvature and the driver. The distribution of the curvature and knowledge about the driver's behaviour also makes it possible to use the model for computer simulations.

It seems, from Figures 14-16, that the effect of the way the driver is driving the vehicle is very important. Although the measurements are performed on the same road, there is a striking difference between the different drivers' behaviour. This appears to be especially pronounced at high acceleration, which is in fact the most important load in terms of fatigue damage.

When the effects of different markets are also applied, as can be seen in Figure 17, the differences between the measurements appear when looking at the number of load cycles at lower lateral accelerations. For instance there is a rather big difference between the numbers of cycles for ranges around $2m/s^2$, while it appears as if the markets have less influence on higher ranges. The fact that the difference is more pronounced for lower lateral acceleration is rather natural since there is a great difference in the number of curves for different roads. (Highways will obviously have fewer curves than urban streets.)

One possible weakness of the model is the difficulty in describing the higher accelerations. It can for instance be seen in Figure 17 that the number of large cycles found in the Brazilian measurement is higher than what the model suggest. This error probably comes from the difficulty in predicting the tails of the distribution for the lateral acceleration. Although most of the accelerations are modelled well, there might very well be an error at the tails. This is especially unfortunate in the case of fatigue when the uppermost loads are the most important. One of the possible reasons for this error can be found in Figure 7, where it can be seen that the errors are, at least to some extent, depending on the curvature. It seems as if the variation increases somewhat as the curvature increases. Another possible reason is that this particular measurement is the one, which has the lowest proportion of two curves in the same direction. The current method, which does not include this proportion, will lead to an overestimate of the total number of cycles and an underestimate of the number of large cycles.

Table 1 shows that the upper bound for the residual signal is relatively large for most measurements, typically being 150-200% of the measured damage. On the other hand the upper bound has the interesting property that it preserves the order of the measurements in terms of damage. This is an important fact since one of the main purposes of the project is to be able to compare the expected damage for different markets.

The problem of overestimation from Table 1 is also an important part of the explanation for the overestimate in Table 2 and Table 3. It can also be seen in Table 2 that the approximation of the damage according to eq. (12) appears to overestimate the damage by a few per cent.

Although deviations from the measurements obviously can be found, it seems as if the model is relatively robust. The most sensitive parts appear to be in the speed model, and possibly also the upper bound for the damage of the residual, where the estimate of the standard deviation of the transformed normal process (σ_{res}) has a big effect on the model. (See eq. (31).) On the other hand it is worth noticing that the measurements are very different in nature and it appears as if the model works well for all measurements studied. It is also important to note that despite the approximations the order of the measurements is still kept in the model.

9. Future Work

The above model gives little insight into the residual signal. It is of great interest to understand what part of the residual comes from the effects of the vehicle, and what part

is due to other effects such as the driver. This can be done by running the trapezoid signal through a simple vehicle model and studying the effects of the signal to see what part of the residual the vehicle is responsible for. Naturally the driver takes into consideration the vehicle responses, but studying the problem as an open loop problem will still lead to some understanding of the loads, not least when it comes to understanding the frequency content.

Another interesting aspect is to include the proportion of two curves in the same direction in the model for the trapezoid acceleration. There might also be a possibility to find at least an asymptotic variance for the damage, and describe the number of curves as a Poisson process, which would give an increased understanding for the variability. A natural way of studying the variability would also be to use parametric bootstrap techniques and simulate sequences.

An important step is also to collect more data. The measured loads studied here only come from a single vehicle. Although tried out in different environments and with different loading conditions and drivers, naturally only a very small part of the possible markets is covered. New techniques for logging signals have been developed over the last couple years and a very interesting aspect of the model is to adapt it to so called on-board logging, which makes it possible to log much larger amounts of data than what is currently possible.

A fourth interesting aspect would be to study the effects of different drivers more closely in order to see if it is possible to find a statistically significant difference between the drivers. In the same way it would be of great interest to study different markets. Another interesting part to be investigated is the robustness of the model. Finally it would of course be of great interest to extend the concept to other loads such as those coming from the topography of the road, and naturally also to continue the work with vertical excitations such as potholes and road vibration.

Acknowledgement

This work has been a joint work between Volvo Truck Corporation, Fraunhofer-Chalmers Research Centre for Industrial Mathematics (FCC), and the Department of Mathematical Statistics at Chalmers University of Technology, where the author is a graduate student. The author wishes to express his gratitude towards his supervisors Dr. Thomas Svensson, FCC, Prof. Jacques de Maré, Chalmers and Dr. Bengt Johannesson, Volvo. Prof. Igor Rychlik also deserves special thanks for reading the manuscript of the second paper and supplying valuable comments, which greatly improved the paper. He also provided the ideas behind large parts of section 6. The project is funded by the Swedish Agency for Innovation Systems.

References

1. Berger, C., Eulitz, K. -G., Heuler, P., Kotte, K. -L., Naundorf, H., Schütz, W., Sonsino, C. M., Wimmer, A., Zenner, H.: Betriebsfestigkeit in Germany – an overview, *International Journal of Fatigue*, Vol. 24, pp. 603-625, 2002.
2. Klemenc, J., Fajdiga, M.: An Improvement to the Methods for Estimating the Statistical Dependencies of the Parameters of Random Load States, *International Journal of Fatigue*, Vol. 26, pp. 141-154, 2004.
3. Grubisic, V., Fischer, G.: Methodology for Effective Design Evaluation and Durability Approval of Car Suspension Components, *SAE Technical Paper 970094*, 1997.
4. Olofsson, M.: *Evaluation of Estimates of Extreme Fatigue Load – Enhanced by Data from Questionnaires*. Licentiate of Engineering Thesis, Chalmers University of Technology, Göteborg, Sweden, 2000.
5. Niemand, L.: *Probabilistic Establishment of Vehicle Fatigue Test Requirements*. Master of Engineering Thesis, University of Pretoria, Pretoria, 1996.
6. Thomas, J.J., Perroud, G., Bignonnet, A., Monnet, D.: Fatigue Design and Reliability in the Automotive Industry. In Marquis, G. Solin, J. (editors), *Fatigue Design and Reliability, ESIS Publication 23*. Oxford, UK: Elsevier Science, pp.1-12, 1999.
7. Edlund, S., Fryk P.O.: The Right Truck for the Job with Global Truck Application Descriptions, *SAE Technical Paper 2004-01-2645*, 2004.
8. Fischer, G.: Design and Quality Assurance of Vehicle Components based on the Usage Related Stress Analysis. *XXIX Convegno Nazionale dell´Associazione Italiana per l'Analisi delle Solleciatazioni*, Lucca, 6-9 Sept. 2000.
9. Dini, A., Rupp, A.: Comparison of Procedures for Experimental and Theoretical Durability Approval of a Truck Axle, *SAE Technical Paper 982787*, 1998.
10. Aurell J., Edlund S.: Operating Severity Distribution a Base for Vehicle Optimization, *11th IAVSD-Symposium on the Dynamics of Vehicles on Roads and Tracks*, Kingston, Canada, 1989.
11. Aurell J., Edlund S.: Prediction of Vibration Environment in Real Operations Described by Q-distributions, *14th IAVSD - Symposium on the Dynamics of Vehicles on Roads and Tracks*, Ann Arbor, USA, 1995.
12. Öijer, F., Edlund, S.: Complete Vehicle Durability Assessments Using Discrete Sets of Random Roads and Transient Obstacles Based on Q-distributions, *17th IAVSD - Symposium on the Dynamics of Vehicles on Roads and Tracks*, Lyngby, Denmark, 2001.
13. Öijer, F., Edlund, S.: Identification of Transient Road Obstacle Distributions and Their Impact on Vehicle Durability and Driver Comfort, *18th IAVSD- Symposium on the Dynamics of Vehicles on Road and Trucks*, Atsugi, Japan, 2003.
14. Vägverket: Vägutformning-94 version S-1, del 6 Linjeföring. *Vägverket Publikation 1994-52*, Borlänge, 1994. (In Swedish).
15. Bauer, O., Mayr, R.: Road Database Design for Velocity Profile Planning, *IEEE Conference on Control Applications – Proceedings*, Istanbul, Turkey, 2003.
16. Karlsson, M.: Driver Independent Road Curve Characterisation, *18th IAVSD- Symposium on the Dynamics of Vehicles on Road and Trucks*, Atsugi, Japan, 2003.
17. Felipe, E., Navin, F.: Automobiles on Horizontal Curves. Experiment and Observations, *Transportation Research Record*, No. 1628, pp. 50-56, 1998.
18. Palmgren, A.: Die Lebensdauer von Kugellagern. *Zeitschrift des Vereins Deutscher Ingenieure*, 68:339-342, 1924.
19. Miner, M.A.: Cumulative Damage in Fatigue, *Journal of Applied Mechanics*, 12:A159-A164, 1945.
20. Dowling, N.E.: Fatigue predictions for complicated stress-strain histories, *Journal of Materials*, 7:71-87, 1972.
21. Endo, T., Mitsunaga, H., Nakagawa, H.: Fatigue of metals subjected to varying stress – prediction of fatigue lives. In *Preliminary Proceedings of the Chugoku-Shikoku District Meeting*, pp. 41-44. The Japanese Society of Mechanical Engineers, November 1967. (In Japanese)
22. Endo, T., Mitsunaga, H., Nakagawa, H., Ikeda, K.: Fatigue of metals subjected to varying stress – low cycle, middle cycle fatigue. In *Preliminary Proceedings of the Chugoku-Shikoku District Meeting*, pp. 41-44. The Japanese Society of Mechanical Engineers, November 1967. (In Japanese)
23. Matsuishi, M., Endo, T.: Fatigue of metals subjected to varying stress, paper presented to Japan Society of Mechanical Engineers, March 1968. (In Japanese)

24. Rychlik, I.: A new definition of the rainflow cycle counting method, *International Journal of Fatigue*, 9:119-121, 1987.
25. Rychlik, I.: Extremes, rainflow cycles and damage functionals in continuous random processes, *Stochastic Processes and their Applications*, Vol 63, pp. 97-116, 1996.
26. Johannesson, P.: Rainflow Cycles for Switching Processes with Markov Structure, *Probability in the Engineering and Informational Sciences*, 12:143-175, 1998.
27. Bishop, N.W.M., Sheratt, F.: A theoretical solution for the estimation of "rainflow" ranges from power spectral density data, *Fatigue and Fracture of Engineering Materials and Structures*, Vol 13, No. 4, pp. 311-326, 1990.
28. Rychlik, I. Rainflow Cycles, Markov Chains and Electrical Circuits, In Spencer, B.F., Johnson, E.A., Balkema, A.A. (editors), *Stochastic Structural Dynamics*, ISBN 90 5809 0248, pp. 229-234, 1999.
29. Samuelsson, J.*: Fatigue Design of Vehicle Components: Methodology and Applications*, PhD Thesis, Royal Institute of Technology, Stockholm, 1988.
30. Schütz, W.: A History of Fatigue. *Engineering Fracture Mechanics*, Vol 54, pp. 263-300, 1996.
31. Johannesson, P., Svensson, T., and de Maré, J.: Fatigue life prediction based on variable amplitude tests - Methodology, *Cumulative Fatigue Damage*, Seville, 2003.

Appendix

A.1. Cumulative fatigue damage

Since this work deals with fatigue loads, there has to be a measure of how damaging the loads are. This measure is the cumulative fatigue damage. It is generally agreed that fatigue is a rate independent process, i.e. the most important properties of the load are the local extreme values and the order of these. Therefore the load can be seen as a sequence of cycles formed by the local extremes. The sequence of cycles must then be transformed into a measure of the cumulative fatigue damage. In order to relate a load sequence to the damage it inflicts the material, some kind of counting method is often used, together with a damage accumulation rule. The accumulated fatigue damage can be calculated for constant amplitude loading with the Wöhler curve, that is

$$N^{-1} = \begin{cases} KS^{\beta}, & S > S_f \\ 0, & S \le S_f \end{cases} \tag{A1}$$

where N is the number of cycles to fatigue failure, and S is the stress amplitude of the applied load. The material parameters are: K, describing the fatigue strength of the material, β, the damage exponent and S_f, the fatigue limit. The next thing is to consider block loading, i.e. blocks of constant amplitude loading one following the other. The Palmgren-Miner rule [18, 19] then states that each cycle with the amplitude S_i uses a fraction $1/N_i$ of the total lifetime. Thus the total fatigue damage is given by

$$D = \sum \frac{n_i}{N_i} \tag{A2}$$

where n_i is the number of cycles with amplitude S_i. Fatigue failure occurs when the damage D exceeds one.

For the more general case of variable amplitude loading, with stress amplitudes $\{S_k\}$, where S_k is the amplitude of the *k*:th cycle, the fatigue damage can be calculated in accordance with the Palmgren-Miner rule as

$$D(T) = \sum_{t_k \le T} \frac{1}{N_{S_k}} \tag{A3}$$

where the sum is extended over all cycles completed at time T. The cycle life N_S can be obtained from $S-N$ data tests with the constant amplitude S. In the same way as above the fatigue failure will occur when $D(T)$ exceeds one. The cycles in this case can be obtained using a number of different cycle counting methods, e.g. the rainflow count method.

Studies have shown that the Palmgren-Miner rule can lead to both conservative and non-conservative results, although the latter is more common. A number of

modifications of the rule have been tried out, carrying names such as relative Palmgren-Miner and Miner consistent. Other approaches have also been used such as the local strain concept. However, neither Samuelsson [29] nor Schütz [30] supports this method. Berger et al. [1] rely more on the relative-Miner, while Schütz [30] who created the method claims the accuracy is insufficient. A generalisation of the relative-Miner was suggested in [31], which is based on variable amplitude testing. Although not tested to a great extent it appears to be a possible way in the future. However, so far it seems as if the simplicity of the Palmgren-Miner rule keeps it in much use. It is also important to keep in mind that the simplification of the load history to accumulated fatigue damage (just one measure) is a rather rough simplification and therefore the models themselves can be rather simple.

In the calculations used in this work the Palmgren-Miner hypothesis will be used together with the commonly used S-N curve

$$N_{S_k}^{-1} = K \cdot S_k^{\beta} \quad \text{with} \quad S_k = \left(M_k - m_k^{rfc}\right) \tag{A4}$$

where M_k and m_k^{rfc} are as in definition 1, and K and β are the parameters in eq. (A1). Since the fatigue limit S_f is dependent of the material we have here for simplicity calculated the results using $S_f = 0$. However, the calculations for arbitrary S_f can of course without any difficulty be studied with the same technique.

A.2. Proof of eq. (27)

Our wish is to show that $\mu_{2n}(u,v) = \frac{n}{2} \cdot \frac{\mathbf{P}(Z > u) \cdot \mathbf{P}(Z > -v)}{\mathbf{P}(Z > u) + \mathbf{P}(Z > -v)}$, where Z is distributed according to eq. (19) or (20), depending on whether we take the extra load into consideration or not. We start with calculating the expected number of up-crossings when $v \le 0 \le u$. For fixed values $v \le 0 \le u$, the expected number of up-crossings of the interval $[v,u]$ can be found as the number of cycles with a minimum below v multiplied with the probability that the sequence exceeds u before going back to v. Denote this probability $p(u,v)$. The expected number of cycles with minimum below v is the expected number of cycles with a minimum below zero multiplied with the probability of having a minimum below v, i.e. $(n/2) \cdot \mathbf{P}(Z > -v)$. We thus get that for fixed $v \le 0 \le u$,

$$\mu_{2n}(u,v) = (n/2) \cdot \mathbf{P}(Z > -v) \cdot p(u,v) \tag{A5}$$

Since the first value after a negative value in the sequence will always be zero, the sequence will in this step be within the interval $[v,u]$. The step after this will either be a step with positive trapezoid acceleration or one with negative each with probability $1/2$. The probability of exceeding u in the first attempt can therefore be calculated as $(1/2) \cdot \mathbf{P}(Z > u)$. However, if the sequence fails to exceed u, but given that it stays within the interval $[v,u]$, there will be another chance with exactly the same probability

of success. (See Figure A1.) The probability for staying in the interval $[v,u]$ is $(1/2)\cdot\mathbf{P}(Z \le u)+(1/2)\cdot\mathbf{P}(-Z \ge v)$. Thus, we can write $p(u,v)$ as

$$p(u,v)=\frac{1}{2}\cdot\mathbf{P}(Z>u)+\frac{1}{2}\cdot[\mathbf{P}(Z\le u)+\mathbf{P}(Z\le -v)]\cdot p(u,v) \tag{A6}$$

which simplifies to

$$p(u,v)=\frac{\mathbf{P}(Z>u)}{\mathbf{P}(Z>u)+\mathbf{P}(Z>-v)} \tag{A7}$$

and hence we see that for fixed values $v \le 0 \le u$ we get using eq. (A7) in eq. (A5) that

$$\mu(u,v)=\frac{n}{2}\cdot\frac{\mathbf{P}(Z>u)\cdot\mathbf{P}(Z>-v)}{\mathbf{P}(Z>u)+\mathbf{P}(Z>-v)}. \tag{A8}$$

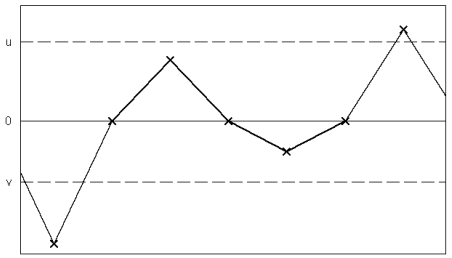

Figure A1. The sequence starts below level v and does not manage to up-cross level u until the third time, but for the points in between the sequence stays in the interval $[v,u]$ so this counts as an up-crossing of the interval.

A.3. Proof of Theorem 3

We would here like to prove that the average number of cycles having range exceeding h could be found as

$$\kappa(h)=n\cdot\frac{\mathbf{P}(Z>h)^2}{1+\mathbf{P}(Z>h)}+\frac{n}{4}-n\cdot\int_{u=0}^{h}\int_{y=0}^{h-u}\frac{\mathbf{P}(Z>u)\cdot\mathbf{P}(Z>y)\cdot g_Z(u)\cdot g_Z(y)}{(\mathbf{P}(Z>u)+\mathbf{P}(Z>y))^3}dydu \tag{A9}$$

As mentioned earlier we have three different types of cycles, one having negative minima and zero maxima, another one having zero minima and positive maxima and the last one having negative minima and positive maxima. We can therefore write $\kappa(h)$ as a sum of the contributions from each of these three cases:

$$\kappa(h)=\kappa_{0,-}(h)+\kappa_{+,0}(h)+\kappa_{+,-}(h) \tag{A10}$$

With the same kind of signal as above with $2n$ points, it was argued that there will on average be $n/2$ positive maxima as well as $n/2$ negative minima. The average number of zero maxima can be found as follows: since the direction of a curve is independent of the direction of the previous one, the probability of having a curve to the left given that the previous one was also to the left is $1/2$. Thus, half of the negative minima will be followed by a zero and then another negative minima. Each such combination leads to a zero local maximum, and thus the average number of zero maxima must be $n/4$. By symmetry it can be argued that the average number of zero minima must also be $n/4$. Since every minima has to be combined with a maxima, and zero minima cannot be combined with zero maxima, we get that there will on average be $n/4$ cycles of each of the three different types of cycles stated above, giving a total of $3n/4$ cycles.

Let us start with considering the cycles with maximum at zero and negative minimum. Let M, m^- and m^+ be as in definition 1. It follows that $H^{rfc}=\min\{m^-,m^+\}$, so assuming that we have a have a cycle with zero maximum, we get

$$\begin{aligned}\mathbf{P}(H^{rfc}>h|M=0)&=\mathbf{P}(\min\{m^-,m^+\}>h|M=0)=\\&=\mathbf{P}(\{m^->h\}\cap\{m^+>h\}|M=0)=\\&=\mathbf{P}(m^->h|M=0)\cdot\mathbf{P}(m^+>h|M=0)\end{aligned} \tag{A11}$$

Definition 1 states that m^+ is the minimum value between the maximum and the nearest point in the forward direction at which the load reaches the maximum. Since we have maximum at zero this will happen immediately after the first minima. Thus we get that

$$\mathbf{P}(m^+>h|M=0)=\mathbf{P}(Z>h) \tag{A12}$$

We are now interested in the first factor i.e. $\mathbf{P}(m^->h|M=0)$. This cannot be found as easily as for the forward direction, since we demand that the load must exceed the maximum in the backward direction. (See definition 1.) We are thus interested if we have at least one local minimum, which goes lower than $-h$ in the backward direction before encountering a maximum above zero. Since the sequence is time-reversible, we can just as well study this as if it would have taken place in the forward direction. Hence, let $p(h)$ denote the probability of down-crossing $-h$ before having a positive local maximum, given that the sequence start at zero and are going down from there. We note that $p(h)=\mathbf{P}(m^->h|M=0)$. The probability of reaching below $-h$ in the first curve is $\mathbf{P}(Z>h)$. If the sequence does not reach below $-h$ then there is probability $1/2$ that the next point will give a minimum, and if it does we are again back in the situation where we started at zero and are going down, and want to find the probability that we are going below $-h$. (See Figure A2.)

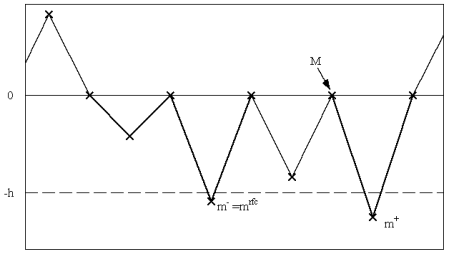

Figure A2. The case with maximum at zero. The first negative value before the maxima does not down-cross the level $-h$, but the second does and hence the range for this cycle is larger than h.

Hence, we can now write $p(h)$ as

$$p(h) = \mathbf{P}(Z > h) + \mathbf{P}(Z \le h) \cdot \frac{1}{2} \cdot p(h) \tag{A13}$$

And rewriting this leads to the following expression:

$$p(h) = \frac{\mathbf{P}(Z > h)}{1 - \frac{1}{2}\mathbf{P}(Z \le h)} = \frac{2 \cdot \mathbf{P}(Z > h)}{1 + \mathbf{P}(Z > h)} \tag{A14}$$

Since we on average have $n/4$ cycles of this type we get, by inserting eq. (A14) and eq. (A12) into eq. (A11), the following result:

$$\kappa_{0,-}(h) = \frac{n}{2} \cdot \frac{\mathbf{P}(Z > h)^2}{1 + \mathbf{P}(Z > h)} \tag{A15}$$

Now assume that we have a cycle with zero minimum. Since we have time reversibility and this case is symmetrical to the one where we had zero maximum it follows that

$$\kappa_{+,0}(h) = \frac{n}{2} \cdot \frac{\mathbf{P}(Z > h)^2}{1 + \mathbf{P}(Z > h)} \tag{A16}$$

For the last case where we have a cycle with positive maximum and negative minimum, note first that since the minima is always negative the range of the rainflow cycle can be seen as the sum of two positive random variables. This follows since $H^{rfc} = M - m^{rfc} = M + \left(-m^{rfc}\right)$, where $M > 0$, and $\left(-m^{rfc}\right) > 0$. In order to find the cumulative probability function for H^{rfc} it is of interest to find the bivariate distribution for the pair $\left(M, -m^{rfc}\right)$. First, note that in this case we have

$$\mathbf{P}\left(M > u, -m^{rfc} > y\right) = \mathbf{P}\left(M > u, m^{rfc} < -y\right) = \frac{\mu_{2n}(u,-y)}{n/4} = 2 \cdot \frac{\mathbf{P}(Z > u) \cdot \mathbf{P}(Z > y)}{\mathbf{P}(Z > u) + \mathbf{P}(Z > y)} \tag{A17}$$

This holds since $\mu_{2n}(u,-y)$ is the expected number of cycles, which have a maximum above u and a minimum below $-y$, when $u \ge 0 \ge -y$, and $n/4$ is the expected number of cycles, which have a maximum above zero and minimum below zero.

The bivariate cumulative distribution function for the pair $\left(M, -m^{rfc}\right)$, i.e. the maximum and minimum can thus be found as

$$\begin{aligned} G(u,y) &= \mathbf{P}\left(M \le u, -m^{rfc} \le y\right) = \\ &= 1 - \mathbf{P}(M > u) - \mathbf{P}\left(-m^{rfc} > y\right) + \mathbf{P}\left(M > u, -m^{rfc} > y\right) = \\ &= 1 - \mathbf{P}(M > u) - \mathbf{P}\left(-m^{rfc} > y\right) + 2 \cdot \frac{\mathbf{P}(Z > u) \cdot \mathbf{P}(Z > y)}{\mathbf{P}(Z > u) + \mathbf{P}(Z > y)} \end{aligned} \tag{A18}$$

Eq. (A18) can now be differentiated with respect to u and y to find the probability density function $g(u,y)$. This leads to the following result:

$$g(u,y) = \frac{\partial^2 G(u,y)}{\partial u \partial y} = 4 \cdot \frac{\mathbf{P}(Z > u) \cdot \mathbf{P}(Z > y) \cdot g_Z(u) \cdot g_Z(y)}{\left[\mathbf{P}(Z > u) + \mathbf{P}(Z > y)\right]^3}, \; u, y \ge 0 \tag{A19}$$

Thus, we can find the cumulative distribution function for the rainflow cycles of this kind as

$$\mathbf{P}\left(H^{rfc} \le h\right) = \int_{u=0}^{h} \int_{y=0}^{h-u} g(u,y)\,dy\,du = \int_{u=0}^{h} \int_{y=0}^{h-u} 4 \cdot \frac{\mathbf{P}(Z > u) \cdot \mathbf{P}(Z > y) \cdot g_Z(u) \cdot g_Z(y)}{\left[\mathbf{P}(Z > u) + \mathbf{P}(Z > y)\right]^3} dy\,du \tag{A20}$$

The probability of a cycle larger than h can simply be found by taking 1 minus the result in eq. (A20). Finally, since we on average have $n/4$ cycles of this type we get

$$\begin{aligned} \kappa_{+,-}(h) &= \frac{n}{4}\left[1 - \mathbf{P}\left(H^{rfc} \le h\right)\right] = \\ &= \frac{n}{4} - n \cdot \int_{u=0}^{h} \int_{y=0}^{h-u} \frac{\mathbf{P}(Z > u) \cdot \mathbf{P}(Z > y) \cdot g_Z(u) \cdot g_Z(y)}{\left[\mathbf{P}(Z > u) + \mathbf{P}(Z > y)\right]^3} dy\,du \end{aligned} \tag{A21}$$

Thus, bringing eq. (A15), eq. (A16) and eq. (A21) together leads to eq. (A9) and we are done with the proof of Theorem 3.

A.4. Proof of Corollary:

For a process $W(t)$ the damage intensity d_W can be found in the following way:

$$d_W = (\text{intensity of cycles}) \cdot K \cdot E\left[\left(H^{rfc}\right)^{\beta}\right], \tag{A22}$$

where β and K are material constants as in the corollary and H^{rfc} is the rainflow amplitude. Rychlik showed in [28] that an upper bound for the different moments $E\left[\left(H^{rfc}\right)^{\beta}\right]$ can be found through the level crossing intensity using the fact that the load can be described as a transformed Gaussian process. (This upper bound also explains the relation between the actual damage and the so-called Rayleigh approximation.) The upper bound for $E\left[\left(H^{rfc}\right)^{\beta}\right]$ is according to [28]:

$$E\left[\left(H^{rfc}\right)^{\beta}\right] \leq \alpha E\left[\left(G(R)-G(-R)\right)^{\beta}\right], \tag{A23}$$

$\beta > 1$, where R is a Rayleigh distributed random variable with the probability density function $f_R(r) = r\exp\left(-r^2/2\right)$, α is the irregularity factor, found as the ratio between the intensity of zero-up-crossings (ν) and the intensity of local maxima, and G is a transformation that transforms a standard Gaussian process ($Z(t)$) into the process of interest. We have in our case that $W(t) = X^2(t)\cdot sign(X(t))$, where $X(t) \in N\left(0,\sigma_{res}^2\right)$, and thus we get that

$$W(t) = X^2(t)\cdot sign(X(t)) = \sigma_{res}^2 \cdot Z^2(t)\cdot sign(Z(t)) = G(Z(t)) \tag{A24}$$

Using the fact that the intensity of cycles has to be equal to the intensity of local maxima, and that a Rayleigh distributed variable is always positive, we can simplify the expression for the damage intensity to:

$$\begin{aligned} d_W &\leq \nu\cdot K\cdot E\left[\left(G(R)-G(-R)^{\beta}\right)\right] = \\ &= \nu\cdot K\cdot E\left[\left(\sigma_{res}^2\cdot R^2\cdot sign(R)-\sigma_{res}^2\cdot(-R)^2\cdot sign(-R)\right)^{\beta}\right] = \\ &= \nu\cdot K\cdot E\left[\left(2\sigma_{res}^2\cdot R^2\right)^{\beta}\right] = \\ &= \nu\cdot K\cdot 2^{\beta}\cdot\sigma_{res}^{2\beta}\cdot E\left[R^{2\beta}\right] \\ &= \nu\cdot K\cdot 2^{2\beta}\cdot\sigma_{res}^{2\beta}\cdot\Gamma(\beta+1) \end{aligned} \tag{A25}$$

where $\Gamma(\cdot)$ is the gamma-function. The last equality holds since the moment for a Rayleigh distributed variable can be found as $E\left[R^k\right] = 2^{k/2}\cdot\Gamma\left(\frac{2+k}{2}\right)$, and hence we get the result in eq. (31).